Wolbachia endosymbionts in two *Anopheles* species indicates independent acquisitions and lack of prophage elements

Shannon Quek[1], Louise Cerdeira[2], Claire L Jeffries[3], Sean Tomlinson[2] Thomas Walker[3*], Grant L. Hughes[1*], Eva Heinz[4*]

[1]Departments of Vector Biology and Tropical Disease Biology, Centre for Neglected Tropical Diseases, Liverpool School of Tropical Medicine, Liverpool, UK

[2]Department of Vector Biology, Liverpool School of Tropical Medicine, Liverpool, UK

[3]Department of Disease Control, Faculty of Infectious and Tropical Diseases, London School of Hygiene and Tropical Medicine, London WC1E 7HT, UK

[4]Departments of Vector Biology and Clinical Sciences, Liverpool School of Tropical Medicine, Liverpool, UK

*Please address correspondence to:

Eva.Heinz@lstmed.ac.uk, Grant.Hughes@lstmed.ac.uk Thomas.Walker@lshtm.ac.uk

Keywords: *Wolbachia*, genomics, *Anopheles*, symbiosis, prophage

Abstract

Wolbachia is a genus of obligate bacterial endosymbionts that infect a diverse range of arthropod species as well as filarial nematodes, with its single described species, *Wolbachia pipientis,* divided into several 'supergroups' based on multilocus sequence typing. *Wolbachia* strains in mosquitoes have been shown to inhibit the transmission of human pathogens including *Plasmodium* malaria parasites and arboviruses. Despite their large host range, *Wolbachia* strains within the major malaria vectors of the *Anopheles (A.) gambiae* and *A. funestus* complexes appear at low density based solely on PCR-based methods. Questions have been raised as to whether this represents a true endosymbiotic relationship. However, recent definitive evidence for two distinct, high-density strains of supergroup B *Wolbachia* within *A. demeilloni* and *A. moucheti* has opened exciting possibilities to explore naturally occurring *Wolbachia* endosymbionts in *Anopheles* for biocontrol strategies to block *Plasmodium* transmission. Here we utilise genomic analyses to demonstrate that both *Wolbachia* strains have retained all key metabolic and transport pathways despite their smaller genome size. We further confirm the presence of cytoplasmic incompatibility factor genes, despite noticeably few prophage regions. Additionally, phylogenetic analysis indicates that these *Wolbachia* strains may have been introduced into these two *Anopheles* species via horizontal transmission events, and unlikely to be by ancestral acquisition and subsequent loss events in the *Anopheles gambiae* species complex. These are the first *Wolbachia* genomes that enable us to study the relationship between natural strains *Plasmodium* malaria parasites and their *Anopheline* hosts.

Impact statement

Wolbachia naturally infects a wide range of arthropod species, including insect vectors of human pathogens, where they may play a role in inhibiting their replication. These bacteria have been commonly found within *Aedes (Ae.) albopictus* and *Culex pipiens* mosquitoes but have been noticeably absent in the *Anopheles* mosquito genera, which includes all species responsible for malaria transmission. Recent PCR-based methods have suggested the potential for natural *Wolbachia* strains

within the *A. gambiae* species complex, which includes major malaria vector species including *A. gambiae* s.s., *A. coluzzii* and *A. arabiensis*. We recently reported the presence of stable *Wolbachia* strains naturally occurring within two different *Anopheles* species (*A. demeilloni* and *A. moucheti)*. In this study, we perform comparative genomic analysis of these two *Wolbachia* genomes against each other and published *Wolbachia* strains. The current assemblies are some of the smallest sequenced *Wolbachia* strains of insects, although their metabolic pathway repertoire is comparable to other strains. Interestingly, prophage fragments were identified within only one of the two strains. The findings of this study will be of significant interest to researchers investigating *Wolbachia* as a potential malaria biocontrol strategy, giving greater insight into the evolution and diversity of this obligate intracellular endosymbiont.

Data summary

Sequence data generated and used for this analysis are available in the National Centre for Biotechnology Information Sequence Read Archive (NCBI SRA bioproject number PRJNA642000). The two assembled *Wolbachia* genomes are available with genome accession numbers GCA_018491735.2 and GCA_018491625.2. Additional *Wolbachia* genomes used for comparative analysis are described in the supplementary material.

The authors confirm all supporting data, code and protocols have been provided within the article or through supplementary data files. Additional supplementary data files used to generate several figures can be found at:
https://figshare.com/projects/Wolbachia_endosymbionts_in_two_Anopheles_species_indicates_independent_acquisitions_and_lack_of_prophage_elements/126533

Introduction

Wolbachia has a wide host range, including insects [1] where various estimates have predicted between 52% to 60% of all arthropod species naturally infected [2, 3]. Attempts to characterise the within-species diversity has resulted in the designation of *Wolbachia* 'supergroups' A through to T [4, 5], with several exceptions [6], via multilocus sequence typing (MLST) of five single-copy conserved genes [7]. The relationship between *Wolbachia* and their hosts can range from obligate mutualism, where the endosymbiont is essential for host survival and reproduction [8, 9], to reproductive parasitism, where it manipulates the reproduction of its host to spread through the population. Currently, the best-studied phenotype (which also affects mosquito hosts) is cytoplasmic incompatibility (CI), which causes infected males to produce unviable offspring unless they mate with an infected female, while infected females have viable offspring regardless of the males infection status, thus conferring a fitness advantage to *Wolbachia*-infected females.

Genetic studies have previously identified a pair of cytoplasmic incompatibility factor genes, *cifA* and *cifB* [10, 11], that have been correlated to this phenotype. These genes have often been found to co-occur as a single operon within prophage Eukaryotic Association Modules (EAMs), and are believed to spread via horizontal transmission between *Wolbachia* strains due to their localisation within prophage regions [12]. Despite being part of the same operon, these genes have been observed to be differentially regulated, with *cif*A having higher expression relative to *cif*B [13]. When these CI genes were first identified, they were placed into three distinct phylogenetic groups. While all three were recognised to maintain protein domains that had predicted nuclease activity, the catalytic residues for these nuclease domains were predicted to be absent in one of the three groups [10], which instead contained an additional protein domain with ubiquitin-like specific protease activity [11, 14, 15]. This was later characterised as the Type I group [14]. Additionally, recent research has identified genes encoding similar features in other members of the *Rickettsiales* order, often found associated with mobile genetic elements, such as plasmids [14, 16]. As a result, a recent study has identified up to five

88 phylogenetic types, with one of these types being identifiable in other *Rickettsia* as well as *Wolbachia*
89 [14].

90 Utilisation of the CI phenotype has been explored as the basis for potential mosquito control strategies
91 to reduce human disease transmission. The bacterium is capable of inducing CI in both natural [5, 17,
92 18] and artificially infected lines [19–21], and possible methods to utilise them for mosquito
93 population control include release of males infected with *Wolbachia* [22], or potentially via release of
94 genetically modified mosquitoes that carry the CI genes, but not *Wolbachia* [23, 24]. In addition to
95 inducing the CI phenotype, *Wolbachia* has been shown to interfere with pathogen replication directly,
96 both in those that cause disease in the insect, as well as human pathogens that utilise the insect as a
97 vector [5, 25–27]. This has been observed to be most effective with artificial infections of *Wolbachia*
98 in non-native host mosquitoes [19–21]. Recent trials have shown that *Wolbachia* can be used to great
99 effect in preventing the spread of dengue virus [28, 29], while laboratory trials have indicated their
100 potential to block *Plasmodium* replication in artificially infected *Anopheles* mosquitoes [30–32]. While
101 there is little evidence to date of stable *Wolbachia* infections [30], a stable infection within *A. stephensi*
102 is possible [31, 32]. Infection of these mosquitoes with *Wolbachia* was associated with significantly
103 reduced hatch rates however [31, 33], possibly affecting the viability of CI as a control tool in this
104 system.

105 Despite *Wolbachia*'s presence in a wide variety of insects, natural high-density strains within the
106 *Anopheles* genus of mosquitoes have not been conclusively proven [34, 35] until recently [36].
107 Previous efforts to detect this bacterium required highly sensitive PCR techniques [37–41] that amplify
108 a select handful of *Wolbachia* genes. Unfortunately, this alone cannot confirm the presence of live
109 bacteria or stable *Wolbachia* strains within insects. Furthermore, phylogenetic placement of these
110 amplified *Wolbachia* sequences within *A. gambiae* shows multiple strains distributed across
111 supergroups A and B, with some strains not assigned to any supergroup [35].

We recently demonstrated high-density *Wolbachia* strains in two *Anopheles* species, *A. demeilloni* and *A. moucheti* [36, 42], which we observed in wild populations collected over a large geographic range in temporally-distinct populations. Importantly, we further visualized these bacteria in the germline, as well as sequenced near-complete *Woblachia* genomes from both host species [36]. Here, we present reassembled and scaffolded genomes for both strains, as well as in-depth comparative analyses of these two *Wolbachia* strains against each other, as well as in the broader context of *Wolbachia* supergroups A through to F, with specific focus on supergroup B. We show that, in terms of both size and predicted protein-coding genes, both assembled genomes are at the low end of the range of *Wolbachia* strains found within insects whilst containing reduced or, in the case of *w*AnM, no prophage WO regions. Despite this, both *Wolbachia* genomes maintained complete pathways that are expected for the genus, such as complete haem and nucleotide biosynthetic pathways and type IV secretion systems. Additionally, we reconstructed the phylogenetic history using whole genome sequence data which indicates that these strains may originate from independent acquisitions via horizontal transfer events, and not from an ancestral infection that has since been lost in other *Anopheles* mosquitoes.

Results

Assembled *Wolbachia* genomes are small in size but supported by high completeness scores

As *Wolbachia* is an obligate intracellular endosymbiont, they have a highly reduced genome and can only be isolated from infected host material, posing a challenge to obtain complete, uncontaminated genome sequences. The updated genome assembly of *Wolbachia* of *A. demeilloni* (*w*AnD) has a total length of 1,231,247 base pairs (bp), while *Wolbachia* of *A. moucheti* (*w*AnM) has a genome length of 1,121,812 bp. While these genome sizes are smaller compared to other analysed *Wolbachia* strains that reside within insects (particularly *w*AnM), they are larger than the genomes of those found in filarial nematodes, which have a maximum size of 1.08 Mbp amongst those compared in our analysis

(Table 1). Refseq annotation of both *w*AnD and *w*AnM genomes identified 1,157 and 1,082 protein-coding genes and 122 and 80 pseudogenes, respectively (Table 1). For comparison, the *Wolbachia* strains of *Ae. albopictus* (*w*AlbB) and *Cx. quinquefasciatus* (*w*Pip) maintained 1,180 and 1,241 protein-coding genes respectively.

As an obligate intracellular endosymbiont that may have multiple strains infecting the same host, assessing *Wolbachia* genome completeness is important to ensure contaminating reads from different strains are not incorporated, and that the assembly does not have significant gaps. Despite the smaller number of protein-coding genes and genome size, both *w*AnD and *w*AnM were noted to contain over 98% of essential single-copy genes as determined by the BUSCO program [43] (Table 1), with only *w*AnM predicted to have one duplicated gene, indicating that both their respective hosts are infected with only a single strain of *Wolbachia*. These figures are in line with previously published and complete *Wolbachia* genomes of strains found within insects (Table 1), with examples such as the *Wolbachia* strains of *Drosophila* flies (*w*Mel, *w*Ri, *w*Ha, *w*Au and *w*No), and mosquitoes (*w*AlbB, *w*Pip) all having completeness scores ranging from 97.5% to 99.5%. Additional details on these genomes and their associated publications used for comparison are available in Supplementary Table 1.

Different *Anopheles* species show potentially independent *Wolbachia* acquisition events

Whole-genome phylogenetic analysis was performed to better understand how *w*AnD and *w*AnM may have been acquired by *Anopheles*, utilising the most closely related genome of *Wolbachia* of *Drosophila (D.) simulans* strain Noumea (*w*No) as a reference [36]. Using a total of 36 genomes of *Wolbachia* strains from supergroup B, a single-nucleotide variant (SNV) alignment of 2,824 base-pairs was generated. The midpoint-rooted tree of the SNV alignment (Figure 1) placed both *w*AnD and *w*AnM within a clade that also includes *w*No, and several *Wolbachia* strains that infect *D. mauritiana* [44–46]. We observed a significant number of differences in this alignment between *w*AnD and *w*AnM strains, with a total of 824 SNVs between the two *Anopheles*-derived strains. By contrast, *w*AnM was

shown to have a total of 408 and 417 SNVs shared between it and the *Wolbachia* strains of *D. mauritiana* and *w*No respectively, suggesting that *w*AnM is more closely related to these strains than to *w*AnD. Additionally, it was observed that *w*AlbB and *w*Pip, two known *Wolbachia* strains of mosquitoes, do not cluster together, and appear in clades separate from both *w*AnM and *w*AnD. This lack of host clustering can be seen throughout the generated phylogenetic tree (Figure 1), with Insecta host members from different orders appearing throughout. Exceptions to this observation come from *Wolbachia* genomes that have been sequenced from the same host, e.g. *Diaphorina citri* or *Drosophila mauritiana*. Such observations are similar to that in previous studies that predict how *Wolbachia* is not solely restricted to vertical transmission ([47, 48]) and could be an indication of independent horizontal acquisition of *w*AnD and *w*AnM in their current hosts, rather than an ancestral infection that has since been lost in other Anopheline mosquitoes. Phylogenetic analysis of COII and ITS2 sequences of *A. demeilloni* and *A. moucheti* indicate significant phylogenetic distances from both the *A. gambiae* and *funestus* complexes [36]. Furthermore, this study also provided no evidence of resident *Wolbachia* strains within *A. marshallii*, a mosquito species closely related to *A. demeilloni* and *moucheti* [36].

The *Wolbachia* core genome is conserved in *w*AnM and *w*AnD orthogroup analysis

Orthologous gene groups are important to identify in *Wolbachia* strains due to their wide distribution across supergroups and diverse hosts, whilst offering insights into the presence/absence of unique pathways that may be involved in host-bacterial symbiosis. For this, we compared the RefSeq annotations of *w*AnD and *w*AnM genomes against 17 *Wolbachia* genomes (Table 1). A total of 18,404 genes were analysed, with 96.8% of these assigned to 1,300 orthogroups, and the remainder left unassigned to any orthogroup. Across the 17 *Wolbachia* strains analysed, a core genome of 9,031 genes distributed across 523 orthogroups was identified (i.e. 40.2% of all identified orthogroups comprising 49.1% of total genes analysed can be considered as part of the core genome, defined as the genes and their protein products that are present in all analysed genomes), with 501 of these orthogroups containing single-copy genes. Outside of this core genome, the number of shared

188 orthogroups is noticeably lower (Figure 2a), and no orthogroups were unique to *Wolbachia*
189 supergroup B strains. For *w*AnD, 18 genes were not assigned to an orthogroup, and no species-specific
190 orthogroups (paralogues present in only one species) were identified (Figure 2a inset). By contrast,
191 *w*AnM was noted to have two species-specific orthogroups containing a total of 47 genes, as well as
192 13 unassigned genes. None of the protein products for these genes had identifiable protein domains.
193 Two orthogroups containing single-copy genes were identified that was specific to both *w*AnD and
194 *w*AnM, although again none of these had identifiable protein domains.

195 Further comparisons were performed using a wider selection of *Wolbachia* supergroup B strains,
196 including eight *Wolbachia* genomes used in the previous analysis, as well as a further 19 draft genomes
197 [44] with over 80% completeness. For consistency, all genomes were annotated using a local
198 installation of NCBI's Prokaryotic Genome Annotation Pipeline (PGAP, [49]). A total of 31,943 genes
199 annotated across the 27 genomes were used, of which 98.4% of these were assigned to 1,678
200 orthogroups (Figure 2b). A core genome (genes and their protein products that are present in all
201 analysed genomes) was identified containing 15,208 genes distributed across 618 orthogroups (47.6%
202 of total genes were assigned to 36.8% of all orthogroups). Of these 618 orthogroups, 177 contain
203 single-copy genes. A total of 34 and 21 genes were not assigned to an orthogroup for *w*AnD and *w*AnM
204 respectively. One species-specific orthogroup was identified in *w*AnD (containing seven genes), and
205 two species-specific orthogroups were identified in *w*AnM (containing 52 genes). Similar to the
206 previous comparison, one orthogroup was identified as specific to both *w*AnD and *w*AnM, containing
207 single-copy orthologues from both genomes that did not have any identifiable protein domains.

208 It was interesting to see that the number of orthogroups that could be considered as part of the core
209 genome is less than 50% for both comparisons conducted here. We observed a total of 90 orthogroups
210 that are not considered 'core' due to their absence within *Wolbachia* strains of filarial nematodes from
211 supergroups C and/or D specifically, whilst supergroup F strains has 30 unique orthogroups.
212 Additionally, the genomes of *Wolbachia* from *D. mauritiana* (*w*Ma and *w*Mau in Figure 2a) shared 26

unique orthogroups. This observation of an extensive accessory genome has been reported in the past, even among closely-related *Wolbachia* strains [50].

Despite smaller genomes, the *Wolbachia* spp. core metabolic pathways are conserved in *w*AnD and *w*AnM

Orthogroup analysis of *w*AnD and *w*AnM indicated a high degree of conservation of supergroup B metabolic capacity, and to confirm this, the KEGG Automatic Annotation Server (KAAS, [51]) was used to assign KEGG Orthology. A total of 677 and 660 protein-coding genes were assigned a KO number for *w*AnD and *w*AnM respectively. Subsequent visualisation and manual annotation identified complete biosynthetic pathways that have previously been considered of interest with respect to *Wolbachia*-host symbiosis (Figure 3a). This includes pathways for riboflavin, purines, pyrimidines and haem biosynthesis; and showed all pathways as present in other supergroup B isolates' genomes. Additionally, both *w*AnD and *w*AnM also contained a suite of metabolite transport and secretion systems common to other *Wolbachia* strains that includes haem, zinc, iron (III), lipoproteins and phospholipids (Figure 3a). This conservation of pathways was also observed when the analysis was focused to only *Wolbachia* from supergroup B strains [44] (Figure 3b). In addition to these biosynthetic pathways, the Type IV and Sec-Secretion systems were also maintained in both *Wolbachia* genomes. The Type IV secretion systems (T4SS) are known to play roles in infection and survival for a diverse range of symbiotic and pathogenic intracellular bacteria [52, 53]. Both *Wolbachia* genomes contained a total of 15 T4SS related genes, organised into two operonic regions and four individual genes spread across the genome. *Wolbachia* strains in the filarial nematode *Brugia malayi* has been predicted to utilise its T4SS to secrete protein effector molecules to avoid autophagy pathways and aid in actin cytoskeleton reformation, allowing intracellular mobility [54]. Such processes may also be conserved within *Wolbachia* strains residing within insects, such as *w*AnD and *w*AnM.

Prophage WO region identification

Wolbachia strains are frequently infected by a bacteriophage known as Phage WO [55], with prophage sequences predicted to be common in the genomes of *Wolbachia* strains of insects [12, 56]. These can be found in various states of completeness depending on the specific strain - some genomes are known to maintain duplicated prophage insertions that can encode a functional phage [57, 58], whilst others have been found to be degenerated [58–60]. By contrast, nematode-specific *Wolbachia* strains are known to have either no, or significantly degraded, prophage sequences [61, 62]. These prophage regions are known to maintain an EAM [63], a group of genes that encode protein domains homologous to those found in eukaryotes. This has resulted in predictions that these genes influence host-*Wolbachia* interactions by mimicking and interacting with host proteins [63]. Additionally, genes that have been implicated in the mode of action for CI have typically been found localised within these prophage EAM regions [10, 11, 15, 63].

In contrast to other *Wolbachia* strains that reside within mosquitoes, *w*AnM contained no prophage fragments identifiable via the PHASTER web server. To confirm this, we aligned the genomes of both *Wolbachia* strains from the two *Anopheles* species to their closest relative, *w*No from *D. simulans*, using the Blast Ring Image Generator (BRIG, [64]). The *Wolbachia* genome of *w*No was previously observed to have four prophage-like regions [58], ranging in size from 5.7 kbp to 47.2 kbp. Initial comparisons of the genomes showed notable gaps within the *w*AnM genome when compared to *w*No, although the same regions appear partially present in *w*AnD (Figure 4a, 4b). Overlaying coordinates for the four prophage regions that were known to be present in *w*No [58] onto this comparison, it was observed that the gaps in alignment with *w*AnM were centred on these *w*No prophage regions (Figure 4a). When the original sequencing reads were mapped to the *w*No genome, we observe very low read coverage on *w*No prophage segments (Supplementary Figure 1), whilst these reads showed even coverage of the *w*AnM genome. This indicates that these prophage regions are not present in the currently assembled genome of *w*AnM.

Within *w*AnD, analysis via the PHASTER web server and subsequent BlastX searches of surrounding regions identified two prophage fragments of lengths 6.3 kbp and 22.1 kbp. BlastX searches also identified an additional prophage-like region of length 11.6 kbp (Figure 4c). The total length of these prophage fragments (approx. 40 kbp) is shorter than published phage WO genomes (lengths of between 55 kbp to 65 kbp, [63, 65]). The two prophage regions identified by PHASTER is predicted to code for a total of 50 genes, 16 of which were predicted to be interrupted by either stop-codons or frameshifts. The prophage-like region identified after manual curation contained 13 genes, of which seven were predicted to be interrupted. Two of these three regions contained structural phage genes that were either intact or interrupted, with examples including phage tail, baseplate, head-tail connectors, and capsid proteins (Supplementary Figure 2).

Cytoplasmic incompatibility (CI) factors are conserved in wAnM and wAnD

We previously reported that the genome of *w*AnD contains one intact pair of *cif* genes (JSQ73_02850, JSQ73_02855), and a second pair which showed interruptions in both genes (JSQ73_02500 through to JSQ73_02515) [36]. In turn, the genome of *w*AnM contains one pair of *cif* genes, although two internal stop codons were identified within *cifB* [36]. Phylogenetic analysis of the concatenated nucleotide sequences of *cifA* and *cifB* identified *w*AnD's intact *cif* gene pair as clustering with the Type I group, and its pseudogenised pair clustering with the Type III group, in line with previous observations [14]. In comparison, the *cif* gene pair of *w*AnM clusters with the Type II group (IYZ83_00740 through to IYZ83_00755, Figure 5).

Within *w*AnD, the interrupted *cif* genes were of a combined 3.6 kbp in length and were located upstream of one of the prophage regions identified by the PHASTER web server (Figure 4c). Following this, the intact *cif* genes of *w*AnD combined measured 6.0 kbp in length, and is approximately 69.5 kbp downstream of the interrupted *cif* genes (Figure 4c). By contrast, the interrupted *cif* genes of wAnM were of a combined 3.6 kbp in length (Figure 4b). Interestingly, none of the three identified pairs of *cif* genes within *w*AnD and *w*AnM were located directly next to or within prophage regions, although

the two within *w*AnD are located close to one (Figure 4c). This is similar to *w*No, whose single intact pair of *cif* genes were observed to be separate from predicted prophage regions (Figure 4a). Additionally, it should be noted that the *cif* gene pair of *w*AnM appear to be a unique insertion that is also not present in *w*AnD (Figure 4b).

Discussion

This study provides a comprehensive analysis of two *Wolbachia* strains recently identified within *Anopheles* mosquitoes. Their high density and prevalence rates within field populations provides an opportunity to better understand *Wolbachia*-host interactions, as well as providing a potential tool to aid in interrupting the spread of *Plasmodium* parasites. One of the first observations from this study is that the *Anopheles*-infecting *Wolbachia* strains are not monophyletic with other *Wolbachia* strains from mosquitoes (*w*AlbB and *w*Pip). Instead, both *w*AnD and *w*AnM were located within a clade that includes several *Wolbachia* strains found within *D. simulans* and *D. mauritiana*. There have been multiple studies that show horizontal transmission of *Wolbachia* occurs regularly [47, 48], and is even possible via a plant intermediate [66]. This potential for horizontal transmission is further emphasised by a recent survey that assembled over 1,000 *Wolbachia* genomes from existing sequence data [44]. These genome assemblies are primarily distributed across various *Wolbachia* strains from supergroups A and B, whilst also generating multiple *Wolbachia* assemblies from the same host [44]. This study observed how closely related *Wolbachia* strains can be found in taxonomically unrelated hosts, as well as finding no meaningful phylogenetic clustering of different hosts and their corresponding resident *Wolbachia* strains. Such observations are similar with what is observed here with the whole-genome phylogeny of *w*AnD and *w*AnM, in relation to the wider supergroup B strains and their insect hosts.

When compared against these other sequenced *Wolbachia* strains, analysis of the *w*AnD and *w*AnM strains indicate that they maintain relatively small genome sizes for strains found within insects. Despite reduced genome sizes, both the *w*AnD and *w*AnM strains maintain similar metabolic and

transport pathways found in other *Wolbachia* strains. Additionally, no biosynthetic pathways were identified that could indicate a previously unknown feature acquired in these two strains found in *Anopheles* mosquitoes. Known pathways of relevance for *Wolbachia* include haem and nucleotide biosynthetic pathways [67], as well as transport components such as the Type IV secretion system for secreting potential protein effectors [52]. The observation of smaller genome sizes could be attributed to a reduced number of mobile elements, specifically prophage regions, when compared to other *Wolbachia* strains that reside in mosquitoes such as *w*AlbB [59] and *w*Pip [57].

Following on from this, it is interesting to see how *w*AnD has degenerated prophage regions in comparison to its closest relative *w*No, whilst *w*AnM lacks prophage regions entirely. This is despite the presence of *cif* genes within both genomes, which are separate from any prophage regions, contrary to previous observations and expectations for these two features to be co-localised [10, 11, 24, 63, 68]. However, this separation of *cif* genes is not unique to just these two *Wolbachia* strains in *Anopheles*, but also to the closely related *Wolbachia* strains *w*No, *w*Ma, and *w*Mau (the first infecting *D. simulans*, the latter two *D. mauritiana*), which have been shown to maintain *cif* genes that are distinctly separate from any prophage WO region [45, 69] (Supplementary Figure 3). It is tempting to speculate that this separation of *cif* genes and prophage regions be a unique feature of this clade of *Wolbachia*. For comparison, the genomes of both *w*AlbB and *w*Pip maintain *cif* genes that are associated with prophage WO regions [10, 59]. In addition to this separation from prophage regions, both strains *w*Ma and *w*Mau were observed to have an interrupted *cif*B gene [45, 69], similar to what is observed in *w*AnM, and are both incapable of inducing CI, but capable of rescuing it, when crossed with *w*No-infected mates [70, 71]. Unlike *w*AnM however, all three of *w*No, *w*Ma and *w*Mau's *cif* gene pairs are found within the Type III phylogenetic group, whereas the *cif* gene pair identified in *w*AnM can be placed within Type II, which is unique amongst this group of five *Wolbachia*. BRIG comparisons of the different genomes appear to indicate this *cif* gene pair to be a unique insertion. Furthermore, whilst *w*AnD's degenerated *cif* gene pair was noted to be a member of the Type III group, its intact *cif* gene pair also appears unique among this group of *Wolbachia* as a member of Type I. Like *w*AnM's

337 sole *cif* gene pair, this intact *cif* gene appears to be a unique insertion event, separate from prophage
338 elements.

339 How such insertion events within both *w*AnD and *w*AnM have come to happen, and where they have
340 come from, is currently an open question that warrants further investigation, alongside how this group
341 of *Wolbachia* maintain *cif* gene pairs that appear separate from identifiable prophage WO regions.
342 One possible explanation is that the recent ancestors for these strains of *Wolbachia* may have
343 acquired these *cif* genes from a recent phage WO insertion that has very recently become degenerated
344 [69]. Alternatively, these prophage regions could have been removed from the genome by phage
345 excision events. Previous publications have discussed what could happen to the *cif* gene pairs, as well
346 as the *Wolbachia* which carry them, once CI is no longer able to induce evolutionary pressure on their
347 hosts [72–75]. For instance, a recent survey of CI genes in *Wolbachia* predicted how, without
348 evolutionary pressure, these CI genes would likely degrade over time, starting with *cif*B, the 'toxin'
349 component of the phenotype, followed by *cif*A, the 'antidote' component [14]. Alternatively, it has
350 also been suggested that the degradation of the *cif* genes may be related to the absence of prophage
351 regions [14, 15], with the former being an adaptation used by the latter to spread within *Wolbachia*
352 populations. Thus, once the prophage regions are removed, it is predicted that the *cif* genes, and thus
353 the CI phenotype, will have no evolutionary pressure to maintain themselves within *Wolbachia* [14,
354 15]. We observe this occurring to some degree in this study, with the dissociation of prophage regions
355 from the *cif* genes, the interrupted Type III pair observed in *w*AnD, and how *w*AnM carries
356 interruptions in its Type II *cif*B gene specifically. Once the phenotype these *Wolbachia* strains exert
357 on their hosts can be properly elucidated, a longitudinal study on the *cif* genes within them is
358 imperative. The results of such study could allow for further insights into *Wolbachia* biology and the
359 evolution of the CI phenotype.

360 Despite the questions as to how this may have occurred, the observed similarities and differences
361 between *w*AnM and its related strains *w*Ma, *w*Mau and *w*No are intriguing, and raises the possibility

that *w*AnM may not cause CI in its *Anopheles* host. This is perhaps counterintuitive, considering the high, but variable, prevalence rates of *w*AnM in field populations of *A. moucheti* [36, 42]. This prevalence rate is a feature shared with *w*AnD [36, 42], which is more likely to be capable of inducing CI due to the presence of intact *cif* genes from the Type I group, of which *w*Mel shares. For comparison, our previous work had shown the prevalence rates of *w*AnM to be between 17.5% and 75%, which is slightly lower than *w*AnD prevalence rates, shown to be between 38.7% and 100%. Yet the ability for *Wolbachia* to persist in ppulations without inducing CI is known, as there are instances of *Wolbachia* which stably infect host populations without any overt reproductive parasitism phenotype [8, 76, 77]. Explanations for this have focused on *Wolbachia* providing some form of fitness benefits to their host. For instance, the Wolbachia strain *w*Au of supergroup A spread through lab-based, uninfected host populations of *D. simulans* without inducing CI [78]. This persistence of *w*Au could be linked to an ability to induce protection against viral infections [79], and it is tempting to speculate that *Wolbachia* may provide protection against pathogens of the mosquito. While such studies focus on *Wolbachia* of supergroup A, there has been some evidence that *w*Mau of supergroup B may also confer a fitness benefit for their host via stimulating egg production [69, 80]. Further research will still need to be done to confirm if *w*AnM can confer similar fitness benefits to its host, or have the potential to inhibit *Plasmodium* or viruses, and whether host-*Wolbachia* backgrounds may play any role in this.

The identification of natural *Wolbachia* infections in *Anopheles* shows promise for future control strategies of *Plasmodium* parasites. Whilst these strains show no pathways that are uniquely present or absent, they do exhibit unusual genomic arrangements with regards to the presence of prophage and *cif* genes. This has potential implications on their relationship with their respective Anopheline hosts, potentially making them good candidates for transinfection into other medically relevant *Anopheles* species, such as *A. gambiae* s.s. Further studies would be required to fully examine these *Wolbachia* strains and elucidate their predicted phenotypes of CI and pathogen blocking, both in the context of natural and artificial associations.

Methods

Sequence data collection and genome quality assessment

Both genomes assemblies of *w*AnD and *w*AnM were manually curated (i.e. gaps, indels and synteny) using the approach described by Tsai and colaborators 2010 [81], Mummer/Nucmer software tool v4.0.0 [82], Mauve v2.4.0 [83] and Tablet v1.21.02.08 [84]. To complement the genomes of *w*AnD and *w*AnM [36], whole genome sequences of 15 *Wolbachia* genomes were downloaded from the National Centre for Biotechnology Information, with these genomes spanning supergroups A through to F (full information available in supplementary table). An additional 25 *Wolbachia* genomes were also downloaded from the European Nucleotide Archive (ENA). These additional genomes were sequenced as part of a large-scale study [44] which looked at assembling *Wolbachia* genomes from a variety of existing sequencing data of various insects. For the 16 published *Wolbachia* genomes downloaded from NCBI, Refseq annotations were obtained via their PGAP [49]. The 25 genomes downloaded from ENA were also annotated using a local installation of PGAP [49], with an additional seven genomes of *Wolbachia* from supergroup B downloaded from NCBI also annotated using this local installation for consistency [49]. The genomes of both *w*AnD and *w*AnM were annotated using both methods. All genome accession numbers used in this study, as well as a summary of their annotations used in this study are provided in supplementary table.

To confirm genome completeness, nucleotide sequences of all downloaded genomes, as well as the assembled genomes of *w*AnD and *w*AnM, were used as input into the programs BUSCO (v5.0.0, [43]) with the lineage option set to “rickettsiales_odb10”. This program analyses genome completeness via comparison against a selection of marker genes (total 364 genes) predicted to be present in single copies based on the input genome’s lineage. Genomes that showed significantly lower completeness levels, (less than 80% completeness) were excluded from orthologue and pathway analyses. This resulted in six of the *Wolbachia* genomes [44] to be removed from these additional analyses.

Phylogenetic, pangenome and metabolic pathway analysis

A total of 34 *Wolbachia* genomes were used for phylogenetic analysis of supergroup B *Wolbachia* (genomes of *w*AnD and *w*AnM, seven *Wolbachia* genomes from NCBI, and 25 from ENA). These genomes were used as input into the program wgsim ([86, 87], version 1.9), which simulates sequencing reads from a genomic template. Base error, mutation, fraction of indels and indel extension probability were set to zero, read lengths set to 100 and a total of ten million reads simulated for each genome. These simulated reads were then used to generate a Single-Nucleotide Variant (SNV) alignment via Snippy v4.6.0 [88] using the *w*No genome as reference (genome accession number GCA_000376585.1). Gubbins v3.0.0 [89] was used for removing recombinant events. Recombination-free alignment of all 34 genomes was then analysed with IQTree v1.6.12 [90] using default parameters, with a GTR substitution model using 1000 non-parametric bootstrap replicates for branch support.

Orthologous group detection

Orthologous group detection was performed in two separate parts- first was to compare coding protein sequences amongst *Wolbachia* of supergroup A through to F, whilst the second was to compare coding protein sequences amongst *Wolbachia* of supergroup B specifically.

For orthologue analysis amongst *Wolbachia* of supergroup A through to F, Refseq protein annotations for the 15 genomes downloaded from NCBI were used, alongside Refseq protein annotations for *w*AnD and *w*AnM. This list of 17 protein sequences were used as input into the program OrthoFinder ([91], v2.5.1) using default parameters. Orthogroups that were common or unique between all 17 *Wolbachia* strains were subsequently plotted using the R program package 'UpsetR' ([92], v1.4.0). Additional querying of the data was then performed using the R program package 'ComplexHeatmaps' ([93], v2.5.5).

For orthologous group detection amongst a wider selection of supergroup B *Wolbachia*, a total of 31 *Wolbachia* genomes were used (seven from NCBI, 22 from ENA), alongside the assembled genomes

436 of *w*AnD and *w*AnM (supplementary table). Protein gene annotations for all *Wolbachia* genomes from
437 a local installation of the NCBI PGAP ([49], build5508 2021-07-01) were used as input into the program
438 Orthofinder ([91], v2.5.1) using default parameters. Orthogroups were again visualised using the R
439 program UpsetR ([92], v1.4.0), with additional data querying performed using the R program
440 ComplexHeatmaps ([93], v2.5.5). Genes of interest identified within these orthogroups, e.g. those that
441 were unique to particular genomes, were further analysed using the PFam website's sequence search
442 [94, 95] and NCBI's BlastP [96]. Comparison of the identified nucleotide regions that had similarity to
443 the *Osmia lignaria* gene XP_034172187.1 was performed by BlastN and BlastX, with visualisations
444 performed using Easyfig [97].

445 Construction of metabolic pathways

446 The genomes of both *w*AnD and *w*AnM were submitted to the NCBI Prokaryotic Annotation Pipeline,
447 with a GenBank Flatfile being generated as a result. This flatfile was then downloaded, and used as
448 input into BioCyc's Pathway Tools program ([98], v24.0) and Pathologic ([99, 100], v24.0). Pathologic
449 is able to assign protein function and pathways to annotated genes based on name and/or automated
450 blast hits. To address proteins with 'ambiguous' function within metabolic pathways, all predicted
451 protein-coding genes of both *w*AnD and *w*AnM were submitted to the EggNOG online server, which
452 allows for the automated transfer of functional annotations ([101], v2.0.1). Predicted protein-coding
453 genes were also submitted to the KEGG Automatic Annotation Server (KAAS, [51], last updated April
454 3rd 2015) as a second method for functional annotation. Any proteins identified by Pathologic as
455 having an 'ambiguous' function was then manually cross-checked with the outputs of EggNOG and
456 KAAS, and enzyme code numbers assigned. This process was repeated for a selection of *Wolbachia*
457 genomes from supergroup B (supplementary table). Once this process was completed, Pathway Tools'
458 Pathway Overview and Comparison options were then used to compare pathways between the
459 different *Wolbachia* strains. A selection of these biosynthetic and transport pathways was then made,
460 based on prior literature investigating their importance to the *Wolbachia*-host endosymbiotic

relationship. Gene presence and absence within these pathways was then manually scored, and plotted out into a heatmap using R's GGplot2 package [102].

Characterisation of *Cytoplasmic Incompatibility Factor* genes

Phylogenetic placement of the three sets of *cif* gene pairs from both *w*AnD and *w*AnM were made following the methods of Martinez *et al.* [14]. Briefly, nucleotide sequences for Cytoplasmic Incompatibility Factor (*cif*) A and B genes for all five monophyletic types were obtained from the supplementary materials of Martinez *et al.* [14]. Partially sequenced *cif* genes were discarded, and the nucleotide sequences for *cif*A and *cif*B genes were aligned separately using the program MAFFT. The separate alignments were then used as input into the online GBlocks server ([103], v0.91b) with default 'stringent' parameters to filter out weakly conserved regions of the alignment. Once filtering was done, the separate nucleotide sequence alignments were then concatenated using Seqkit ([104], v0.15.0), and used as input for PhyML ([105], v3.0), using the GTR GAMMA substitution model of evolution and 1,000 bootstrap replicates. The outputted newick formatted tree was then annotated using the GGTree package in R ([106], v2.2.4).

Ankyrin, Prophage and IS element detection

Ankyrin domains were detected using five HMMer profiles ([95], ID numbers PF00023.31, PF12796.8, PF13606.7, PF13637.7, PF13857.7). These profiles were generated via first downloading associated alignment files from the PFAM protein database [94] as Stockholm formatted seed files. The HMMer suite ([95], v3.1b2) was then used to build HMM profiles from these seed files. These profiles were then compared against the protein amino acid sequences annotated from *w*AnD and *w*AnM to identify any protein-coding genes containing an ankyrin domain. This analysis was then repeated for a selection of *Wolbachia* genomes to allow for direct comparisons to be made.

Prophage sequences were identified within the genomes of *w*AnD and *w*AnM using the PHASTER web server [107]. Assembled contig sequences of both genomes were uploaded separately to the server, checking the option to note that the input consists of multiple separate contigs. In the case of *w*AnD

where prophage regions were detected, results were downloaded and manual curation of the identified prophage regions was performed using the Artemis genome browser [108] to identify prophage genes overlapping these regions. Additional BlastX searches were performed on neighbouring genes against Phage WOVitA1 sequences (GenBank genome reference HQ906662.1) to screen for genes that may be associated with prophage WO's eukaryotic association module.

Insertion sequence element detection was performed by separately concatenating the contigs of *w*AnD and *w*AnM, resulting in two contiguous genomes. These were then submitted to ISSaga ([109], v1.0) and results tables obtained. Manual curation was then performed using the original contigs for both *Wolbachia* genomes, with true-positive IS elements called by comparison of annotations from ISSaga, PGAP annotation, and BLAST searches against the ISFinder database.

Author statements

S.Q. designed methodology, conduct investigation and formal analysis, designed visuals, and wrote the original draft. L.C. designed methodology, conduct investigation and formal analysis, and wrote the original draft. C.L.J. conceptualised the study, conducted investigation and resource collection, and wrote the original draft. S.T. designed methodology and software. T.W. conceptualised the study, conducted investigation and resource collection, secured funding, and wrote the original draft. G.L.H. conceptualised and supervised the study, secured funding, and wrote the original draft. E.H. conceptualised and supervised the study, designed the methodology, and wrote the original draft. All authors have read and approved the final manuscript.

The authors declare that there are no conflicts of interest.

509 **Funding information**

510 EH and GLH acknowledge support from BBSRC grant BB/V011278/1. ST was supported by the
511 Wellcome SEED award 217303/Z/19/Z to EH. LC was supported by NIAID R01-AI116811. TW and CLJ
512 were supported by a Sir Henry Dale Wellcome Trust/Royal Society fellowship awarded to TW
513 (101285): https://wellcome.org and https://royalsociety.org. TW was also supported by a Royal
514 Society challenge grant (CHG\R1\170036). GLH was also supported by the BBSRC (BB/T001240/1), a
515 Royal Society Wolfson Fellowship (RSWF\R1\180013), the NIH (R21AI138074), the EPSRC
516 (EP/V043811/1), the UKRI (20197 and 85336), and the NIHR (NIHR2000907).

517

References

1. **Werren JH, Baldo L, Clark ME**. Wolbachia: Master manipulators of invertebrate biology. *Nat Rev Microbiol* 2008;6:741–751.

2. **Weinert LA, Araujo-Jnr E V., Ahmed MZ, Welch JJ**. The incidence of bacterial endosymbionts in terrestrial arthropods. *Proc R Soc B Biol Sci* 2015;282:3–8.

3. **Sazama EJ, Bosch MJ, Shouldis CS, Ouellette SP, Wesner JS**. Incidence of Wolbachia in aquatic insects. *Ecol Evol* 2017;7:1165–1169.

4. **Taylor MJ, Bordenstein SR, Slatko B**. Microbe Profile : Wolbachia : a sex selector , a viral protector and a target to treat filarial nematodes. *Microbiology* 2019;1345–1347.

5. **Kaur R, Shropshire JD, Cross KL, Leigh B, Mansueto AJ, *et al.*** Living in the endosymbiotic world of Wolbachia: A centennial review. *Cell Host Microbe* 2021;29:879–893.

6. **Baldo L, Werren JH**. Revisiting Wolbachia Supergroup Typing Based on WSP: Spurious Lineages and Discordance with MLST. *Curr Microbiol* 2007;55:81–87.

7. **Baldo L, Hotopp JCD, Jolley KA, Bordenstein SR, Biber SA, *et al.*** Multilocus sequence typing system for the endosymbiont Wolbachia pipientis. *Appl Environ Microbiol* 2006;72:7098–7110.

8. **Hosokawa T, Koga R, Kikuchi Y, Meng X-Y, Fukatsu T**. Wolbachia as a bacteriocyte-associated nutritional mutualist. *Proc Natl Acad Sci* 2010;107:769–774.

9. **Nikoh N, Hosokawa T, Moriyama M, Oshima K, Hattori M, *et al.*** Evolutionary origin of insect-Wolbachia nutritional mutualism. *Proc Natl Acad Sci* 2014;111:10257–10262.

10. **Le Page DP, Metcalf JA, Bordenstein SR, On J, Perlmutter JI, *et al.*** Prophage WO genes recapitulate and enhance Wolbachia-induced cytoplasmic incompatibility. *Nature* 2017;543:243–247.

11. **Beckmann JF, Ronau JA, Hochstrasser M**. A Wolbachia deubiquitylating enzyme induces cytoplasmic incompatibility. *Nat Microbiol* 2017;2:1–7.

12. **Bordenstein SR, Wernegreen JJ**. Bacteriophage flux in endosymbionts (Wolbachia): Infection frequency, lateral transfer, and recombination rates. *Mol Biol Evol* 2004;21:1981–1991.

13. **Lindsey ARI, Rice DW, Bordenstein SR, Brooks AW, Bordenstein SR, *et al.*** Evolutionary Genetics of Cytoplasmic Incompatibility Genes cifA and cifB in Prophage WO of Wolbachia. *Genome Biol Evol* 2018;10:434–451.

14. **Martinez J, Klasson L, Welch JJ, Jiggins FM**. Life and Death of Selfish Genes: Comparative Genomics Reveals the Dynamic Evolution of Cytoplasmic Incompatibility. *Mol Biol Evol*. Epub ahead of print 2020. DOI: 10.1093/molbev/msaa209.

15. **Beckmann JF, Bonneau M, Chen H, Hochstrasser M, Poinsot D, *et al.*** The Toxin–Antidote Model of Cytoplasmic Incompatibility: Genetics and Evolutionary Implications. *Trends Genet* 2019;35:175–185.

16. **Gillespie JJ, Driscoll TP, Verhoeve VI, Rahman MS, Macaluso KR, *et al.*** A tangled web: Origins of reproductive parasitism. *Genome Biol Evol* 2018;10:2292–2309.

17. **Werren JH**. Biology of Wolbachia. *Annu Rev Entomol* 1997;124:587–609.

18. **Serbus LR, Casper-Lindley C, Landmann F, Sullivan W**. The Genetics and Cell Biology of *Wolbachia* -Host Interactions. *Annu Rev Genet* 2008;42:683–707.

19. **McMeniman CJ, Lane R V., Cass BN, Fong AWC, Sidhu M, *et al.*** Stable introduction of a life-shortening Wolbachia infection into the mosquito Aedes aegypti. *Science (80-)* 2009;323:141–144.

20. **Walker T, Johnson PH, Moreira LA, Iturbe-Ormaetxe I, Frentiu FD, *et al.*** The wMel Wolbachia strain blocks dengue and invades caged Aedes aegypti populations. *Nature* 2011;476:450–453.

21. **Hoffmann AA, Montgomery BL, Popovici J, Iturbe-Ormaetxe I, Johnson PH, *et al.*** Successful establishment of Wolbachia in Aedes populations to suppress dengue transmission. *Nature* 2011;476:454–459.

22. **Crawford JE, Clarke DW, Criswell V, Desnoyer M, Cornel D, *et al.*** Efficient production of male Wolbachia-infected Aedes aegypti mosquitoes enables large-scale suppression of wild populations. *Nat Biotechnol* 2020;38:482–492.

23. **Shropshire JD, On J, Layton EM, Zhou H, Bordenstein SR**. One prophage WO gene rescues cytoplasmic incompatibility in Drosophila melanogaster. *Proc Natl Acad Sci* 2018;115:4987–4991.

24. **Shropshire JD, Bordenstein SR**. Two-By-One model of cytoplasmic incompatibility: Synthetic recapitulation by transgenic expression of cifA and cifB in Drosophila. *PLOS Genet* 2019;15:e1008221.

25. **McGraw EA, O'Neill SL**. Beyond insecticides: New thinking on an ancient problem. *Nat Rev Microbiol* 2013;11:181–193.

26. **Bourtzis K, Dobson SL, Xi Z, Rasgon JL, Calvitti M, *et al.*** Harnessing mosquito-Wolbachia symbiosis for vector and disease control. *Acta Trop* 2014;132:S150–S163.

27. **Johnson KN**. The impact of Wolbachia on virus infection in mosquitoes. *Viruses* 2015;7:5705–5717.

28. **Utarini A, Indriani C, Ahmad RA, Tantowijoyo W, Arguni E, *et al.*** Efficacy of Wolbachia-Infected Mosquito Deployments for the Control of Dengue. *N Engl J Med* 2021;384:2177–2186.

29. **Indriani C, Tantowijoyo W, Rancès E, Andari B, Prabowo E, *et al.*** Reduced dengue incidence following deployments of Wolbachia -infected Aedes aegypti in Yogyakarta , Indonesia : a quasi-experimental trial using controlled interrupted time series analysis. *Gates Open Res* 2020;1–13.

30. **Hughes GL, Koga R, Xue P, Fukatsu T, Rasgon JL**. Wolbachia infections are virulent and inhibit the human malaria parasite Plasmodium falciparum in Anopheles gambiae. *PLoS Pathog* 2011;7:3–10.

31. **Bian G, Joshi D, Dong Y, Lu P, Zhou G, *et al.*** Wolbachia invades Anopheles stephensi populations and induces refractoriness to Plasmodium infection. *Science (80-)* 2013;340:748–751.

32. **Joshi D, Pan X, McFadden MJ, Bevins D, Liang X, *et al.*** The maternally inheritable Wolbachia wAlbB induces refractoriness to Plasmodium berghei in Anopheles stephensi. *Front Microbiol* 2017;8:1–11.

33. **Joshi D, McFadden MJ, Bevins D, Zhang F, Xi Z**. Wolbachia strain wAlbB confers both fitness

600 costs and benefit on Anopheles stephensi. *Parasites and Vectors* 2014;7:1–9.

601 34. **Walker T, Moreira LA**. Can Wolbachia be used to control malaria? *Mem Inst Oswaldo Cruz*
602 2011;106:212–217.

603 35. **Chrostek E, Gerth M**. Is Anopheles gambiae a Natural Host of Wolbachia ? *MBio* 2019;10:1–
604 10.

605 36. **Walker T, Quek S, Jeffries CL, Bandibabone J, Dhokiya V, *et al.*** Stable high-density and
606 maternally inherited Wolbachia infections in Anopheles moucheti and Anopheles demeilloni
607 mosquitoes. *Curr Biol* 2021;2020.10.29.357400.

608 37. **Baldini F, Segata N, Pompon J, Marcenac P, Shaw WR, *et al.*** Evidence of natural Wolbachia
609 infections in field populations of Anopheles gambiae. *Nat Commun* 2014;1–7.

610 38. **Gomes FM, Hixson BL, Tyner MDW, Ramirez JL, Canepa GE, *et al.*** Effect of naturally
611 occurring Wolbachia in Anopheles gambiae s.l. mosquitoes from Mali on Plasmodium
612 falciparum malaria transmission. *Proc Natl Acad Sci U S A* 2017;114:12566–12571.

613 39. **Niang EHA, Bassene H, Makoundou P, Fenollar F, Weill M, *et al.*** First report of natural
614 Wolbachia infection in wild Anopheles funestus population in Senegal. *Malar J* 2018;17:1–6.

615 40. **Ayala D, Akone-Ella O, Rahola N, Kengne P, Ngangue MF, *et al.*** Natural Wolbachia infections
616 are common in the major malaria vectors in Central Africa. *Evol Appl* 2019;12:1583–1594.

617 41. **Wong ML, Liew JWK, Wong WK, Pramasivan S, Mohamed Hassan N, *et al.*** Natural
618 Wolbachia infection in field-collected Anopheles and other mosquito species from Malaysia.
619 *Parasit Vectors* 2020;13:414.

620 42. **Jeffries CL, Lawrence GG, Golovko G, Kristan M, Orsborne J, *et al.*** Novel Wolbachia strains in
621 Anopheles malaria vectors from Sub-Saharan Africa. *Wellcome Open Res* 2018;3:113.

622 43. **Simão FA, Waterhouse RM, Ioannidis P, Kriventseva E V., Zdobnov EM**. BUSCO: Assessing
623 genome assembly and annotation completeness with single-copy orthologs. *Bioinformatics*
624 2015;31:3210–3212.

625 44. **Scholz M, Albanese D, Tuohy K, Donati C, Segata N, *et al.*** Large scale genome
626 reconstructions illuminate Wolbachia evolution. *Nat Commun* 2020;11:5235.

627 45. **Baião GC, Janice J, Galinou M, Klasson L**. Comparative Genomics Reveals Factors Associated
628 with Phenotypic Expression of Wolbachia. *Genome Biol Evol* 2021;13:1–20.

629 46. **Lefoulon E, Vaisman N, Frydman HM, Sun L, Foster JM, *et al.*** Large Enriched Fragment
630 Targeted Sequencing (LEFT-SEQ) Applied to Capture of Wolbachia Genomes. *Sci Rep* 2019;1–
631 10.

632 47. **O'Neill SL, Giordano R, Colbert AME, Karr TL, Robertson HM**. 16S rRNA phylogenetic analysis
633 of the bacterial endosymbionts asociated with cytoplasmic incompatibility in insects. *Proc*
634 *Natl Acad Sci U S A* 1992;89:2699–2702.

635 48. **Werren JH, Zhang W, Guo LR**. Evolution and phylogeny of Wolbachia : reproductive parasites
636 of arthropods. *Proc R Soc London Ser B Biol Sci* 1995;261:55–63.

637 49. **Tatusova T, Dicuccio M, Badretdin A, Chetvernin V, Nawrocki EP, *et al.*** NCBI prokaryotic
638 genome annotation pipeline. *Nucleic Acids Res* 2016;44:6614–6624.

639 50. **Ishmael N, Hotopp JCD, Loanidis P, Biber S, Sakamoto J, *et al.*** Extensive genomic diversity of
640 closely related wolbachia strains. *Microbiology* 2009;155:2211–2222.

641 51. **Moriya Y, Itoh M, Okuda S, Yoshizawa AC, Kanehisa M**. KAAS: An automatic genome
642 annotation and pathway reconstruction server. *Nucleic Acids Res* 2007;35:182–185.

643 52. **Rancès E, Voronin D, Tran-Van V, Mavingui P**. Genetic and functional characterization of the
644 type IV secretion system in Wolbachia. *J Bacteriol* 2008;190:5020–5030.

645 53. **Christie PJ, Whitaker N, González-Rivera C**. Mechanism and structure of the bacterial type IV
646 secretion systems. *Biochim Biophys Acta - Mol Cell Res* 2014;1843:1578–1591.

647 54. **Carpinone EM, Li Z, Mills MK, Foltz C, Brannon ER, *et al.*** Identification of putative effectors
648 of the type IV secretion system from the wolbachia endosymbiont of brugia malayi. *PLoS One*
649 2018;13:1–24.

650 55. **Kent BN, Bordenstein SR**. Phage WO of Wolbachia: Lambda of the endosymbiont world.
651 *Trends Microbiol* 2010;18:173–181.

652 56. **Gavotte L, Henri H, Stouthamer R, Charif D, Charlat S, *et al.*** A survey of the bacteriophage
653 WO in the endosymbiotic bacteria Wolbachia. *Mol Biol Evol* 2007;24:427–435.

654 57. **Klasson L, Walker T, Sebaihia M, Sanders MJ, Quail MA, *et al.*** Genome Evolution of
655 Wolbachia Strain wPip from the Culex pipiens Group. *Mol Biol Evol* 2008;25:1877–1887.

656 58. **Ellegaard KM, Klasson L, Näslund K, Bourtzis K, Andersson SGE**. Comparative Genomics of
657 Wolbachia and the Bacterial Species Concept. *PLoS Genet*;9. Epub ahead of print 2013. DOI:
658 10.1371/journal.pgen.1003381.

659 59. **Sinha A, Li Z, Sun L, Carlow CKS, Cordaux R**. Complete Genome Sequence of the Wolbachia
660 wAlbB Endosymbiont of Aedes albopictus. *Genome Biol Evol* 2019;11:706–720.

661 60. **Miao YH, Xiao JH, Huang DW**. Distribution and Evolution of the Bacteriophage WO and Its
662 Antagonism With Wolbachia. *Front Microbiol* 2020;11:1–13.

663 61. **Foster J, Ganatra M, Kamal I, Ware J, Makarova K, *et al.*** The Wolbachia genome of Brugia
664 malayi: Endosymbiont evolution within a human pathogenic nematode. *PLoS Biol*
665 2005;3:0599–0614.

666 62. **Lefoulon E, Clark T, Guerrero R, Cañizales I, Cardenas-Callirgos JM, *et al.*** Diminutive,
667 degraded but dissimilar: Wolbachia genomes from filarial nematodes do not conform to a
668 single paradigm. *Microb Genomics* 2020;3:1–45.

669 63. **Bordenstein SR, Bordenstein SR**. Eukaryotic association module in phage WO genomes from
670 Wolbachia. *Nat Commun* 2016;7:1–10.

671 64. **Alikhan NF, Petty NK, Ben Zakour NL, Beatson SA**. BLAST Ring Image Generator (BRIG):
672 Simple prokaryote genome comparisons. *BMC Genomics*;12. Epub ahead of print 2011. DOI:
673 10.1186/1471-2164-12-402.

674 65. **Kupritz J, Martin J, Fischer K, Curtis KC, Fauver JR, *et al.*** Isolation and characterization of a
675 novel bacteriophage WO from Allonemobius socius crickets in Missouri. *PLoS One*
676 2021;16:e0250051.

677 66. **Chrostek E, Pelz-Stelinski K, Hurst GDD, Hughes GL**. Horizontal transmission of intracellular
678 insect symbionts via plants. *Front Microbiol* 2017;8:1–8.

679 67. **Gill AC, Darby AC, Makepeace BL**. Iron Necessity: The Secret of Wolbachia's Success? *PLoS*
680 *Negl Trop Dis*;8. Epub ahead of print 2014. DOI: 10.1371/journal.pntd.0003224.

681 68. **Shropshire JD, Rosenberg R, Bordenstein SR**. The impacts of cytoplasmic incompatibility

682 factor (cifA and cifB) genetic variation on phenotypes. *Genetics*;217. Epub ahead of print
683 2021. DOI: 10.1093/GENETICS/IYAA007.

684 69. **Meany MK, Conner WR, Richter S V., Bailey JA, Turelli M, *et al.*** Loss of cytoplasmic
685 incompatibility and minimal fecundity effects explain relatively low Wolbachia frequencies in
686 Drosophila mauritiana. *Evolution (N Y)* 2019;73:1278–1295.

687 70. **Bourtzis K, Dobson SL, Braig HR, O'Neill SL**. Rescuing Wolbachia have been overlooked¨. .
688 *Nature* 1998;391:852–853.

689 71. **Charlat S, Le Chat L, Merçot H**. Characterization of non-cytoplasmic incompatibility inducing
690 Wolbachia in two continental African populations of Drosophila simulans. *Heredity (Edinb)*
691 2003;90:49–55.

692 72. **Turelli M**. Evolution of incompatibility-inducing microbes and their hosts. *Evolution (N Y)*
693 1994;48:1500–1513.

694 73. **Hurst LD, McVean GT**. Clade selection, reversible evolution and the persistence of selfish
695 elements: The evolutionary dynamics of cytoplasmic incompatibility. *Proc R Soc B Biol Sci*
696 1996;263:97–104.

697 74. **Koehcke A, Telschow A, Werren JH, Hammerstein P**. Life and death of an influential
698 passenger: Wolbachia and the evolution of CI-modifiers by their hosts. *PLoS One*;4. Epub
699 ahead of print 2009. DOI: 10.1371/journal.pone.0004425.

700 75. **Haygood R, Turelli M**. Evolution of incompatibility-inducing microbes in subdivided host
701 populations. *Evolution (N Y)* 2009;63:432–447.

702 76. **Dedeine F, Boulétreau M, Vavre F**. Wolbachia requirement for oogenesis: Occurrence within
703 the genus Asobara (Hymenoptera, Braconidae) and evidence for intraspecific variation in A.
704 tabida. *Heredity (Edinb)* 2005;95:394–400.

705 77. **Kriesner P, Hoffmann AA, Lee SF, Turelli M, Weeks AR**. Rapid Sequential Spread of Two
706 Wolbachia Variants in Drosophila simulans. *PLoS Pathog*;9. Epub ahead of print 2013. DOI:
707 10.1371/journal.ppat.1003607.

708 78. **Kriesner P, Hoffmann AA**. Rapid spread of a Wolbachia infection that does not affect host
709 reproduction in Drosophila simulans cage populations. *Evolution (N Y)* 2018;72:1475–1487.

710 79. **Ant TH, Herd CS, Geoghegan V, Hoffmann AA, Sinkins P**. The Wolbachia strain w Au provides
711 highly efficient virus transmission blocking in Aedes aegypti. 2018;1–19.

712 80. **Fast EM, Toomey ME, Panaram K, Desjardins D, Kolaczyk ED, *et al.*** Wolbachia enhance
713 Drosophila stem cell proliferation and target the germline stem cell niche. *Science (80-)*
714 2011;334:990–992.

715 81. **Tsai IJ, Otto TD, Berriman M**. Improving draft assemblies by iterative mapping and assembly
716 of short reads to eliminate gaps. *Genome Biol*;11. Epub ahead of print 2010. DOI: 10.1186/gb-
717 2010-11-4-r41.

718 82. **Marçais G, Delcher AL, Phillippy AM, Coston R, Salzberg SL, *et al.*** MUMmer4: A fast and
719 versatile genome alignment system. *PLoS Comput Biol* 2018;14:1–14.

720 83. **Darling ACE, Mau B, Blattner FR, Perna NT**. Mauve: Multiple Alignment of Conserved
721 Genomic Sequence With Rearrangements. *Genome Res* 2004;14:1394–1403.

722 84. **Milne I, Stephen G, Bayer M, Cock PJA, Pritchard L, *et al.*** Using tablet for visual exploration
723 of second-generation sequencing data. *Brief Bioinform* 2013;14:193–202.

85. **Seemann T**. Prokka: Rapid prokaryotic genome annotation. *Bioinformatics* 2014;30:2068–2069.

86. **Li H**. Wgsim for simulating sequence reads from a reference genome. https://github.com/lh3/wgsim (2011).

87. **Li H, Handsaker B, Wysoker A, Fennell T, Ruan J, *et al.*** The Sequence Alignment/Map format and SAMtools. *Bioinformatics* 2009;25:2078–2079.

88. **Seeman T**. Snippy: Fast bacterial variant calling from NGS reads. https://github.com/tseemann/snippy (2015).

89. **Croucher NJ, Page AJ, Connor TR, Delaney AJ, Keane JA, *et al.*** Rapid phylogenetic analysis of large samples of recombinant bacterial whole genome sequences using Gubbins. *Nucleic Acids Res* 2015;43:e15.

90. **Nguyen LT, Schmidt HA, Von Haeseler A, Minh BQ**. IQ-TREE: A fast and effective stochastic algorithm for estimating maximum-likelihood phylogenies. *Mol Biol Evol* 2015;32:268–274.

91. **Emms DM, Kelly S**. OrthoFinder: solving fundamental biases in whole genome comparisons dramatically improves orthogroup inference accuracy. *Genome Biol* 2015;16:157.

92. **Conway JR, Lex A, Gehlenborg N**. UpSetR: An R package for the visualization of intersecting sets and their properties. *Bioinformatics* 2017;33:2938–2940.

93. **Gu Z, Eils R, Schlesner M**. Complex heatmaps reveal patterns and correlations in multidimensional genomic data. *Bioinformatics* 2016;32:2847–2849.

94. **El-Gebali S, Mistry J, Bateman A, Eddy SR, Luciani A, *et al.*** The Pfam protein families database in 2019. *Nucleic Acids Res* 2019;47:D427–D432.

95. **Howard Hughes Medical Institute**. HMMER: biosequence analysis using profile hidden Markov models. http://hmmer.org/ (2013).

96. **Altschul SF, Gish W, Miller W, Myers EW, Lipman DJ**. Basic local alignment search tool. *J Mol Biol* 1990;215:403–10.

97. **Sullivan MJ, Petty NK, Beatson SA**. Easyfig: A genome comparison visualizer. *Bioinformatics* 2011;27:1009–1010.

98. **Karp PD, Midford PE, Billington R, Kothari A, Krummenacker M, *et al.*** Pathway Tools version 23.0 update: software for pathway/genome informatics and systems biology. *Brief Bioinform* 2021;22:109–126.

99. **Caspi R, Billington R, Keseler IM, Kothari A, Krummenacker M, *et al.*** The MetaCyc database of metabolic pathways and enzymes-a 2019 update. *Nucleic Acids Res* 2020;48:D455–D453.

100. **Karp PD, Billington R, Caspi R, Fulcher CA, Latendresse M, *et al.*** The BioCyc collection of microbial genomes and metabolic pathways. *Brief Bioinform* 2018;20:1085–1093.

101. **Huerta-Cepas J, Forslund K, Coelho LP, Szklarczyk D, Jensen LJ, *et al.*** Fast genome-wide functional annotation through orthology assignment by eggNOG-mapper. *Mol Biol Evol* 2017;34:2115–2122.

102. **Wickham H**. *ggplot2: Elegant Graphics for Data Analysis*. New York: Springer-Verlag. https://ggplot2.tidyverse.org (2016).

103. **Talavera G, Castresana J**. Improvement of phylogenies after removing divergent and ambiguously aligned blocks from protein sequence alignments. *Syst Biol* 2007;56:564–577.

765 104. **Shen W, Le S, Li Y, Hu F**. SeqKit: A Cross-Platform and Ultrafast Toolkit for FASTA/Q File
766 Manipulation. *PLoS One* 2016;11:e0163962.

767 105. **Guindon S, Dufayard JF, Lefort V, Anisimova M, Hordijk W, *et al.*** New algorithms and
768 methods to estimate maximum-likelihood phylogenies: Assessing the performance of PhyML
769 3.0. *Syst Biol* 2010;59:307–321.

770 106. **Yu G, Smith DK, Zhu H, Guan Y, Lam TTY**. Ggtree: an R Package for Visualization and
771 Annotation of Phylogenetic Trees With Their Covariates and Other Associated Data. *Methods*
772 *Ecol Evol* 2017;8:28–36.

773 107. **Arndt D, Grant JR, Marcu A, Sajed T, Pon A, *et al.*** PHASTER : a better, faster version of the
774 PHAST phage search tool. *Nucleic Acids Res* 2016;44:16–21.

775 108. **Carver T, Harris SR, Berriman M, Parkhill J, McQuillan JA**. Artemis: An integrated platform for
776 visualization and analysis of high-throughput sequence-based experimental data.
777 *Bioinformatics* 2012;28:464–469.

778 109. **Varani AM, Siguier P, Gourbeyre E, Charneau V, Chandler M**. ISsaga is an ensemble of web-
779 based methods for high throughput identification and semi-automatic annotation of insertion
780 sequences in prokaryotic genomes. *Genome Biol*;12. Epub ahead of print 2011. DOI:
781 10.1186/gb-2011-12-3-r30.

782

Figures

***Figure 1*: Maximum likelihood phylogenetic tree of whole-genome alignments of a selection of *Wolbachia* genomes, using 1000 bootstrap replicates.** Genomes beginning with WOLB followed by four digits were assembled by [44]. Other genomes, with the exception of *w*AnM and *w*AnD (which are bolded and underlined) are the results of previous sequencing efforts, with acronyms as described in Table 1. Tree is midpoint-rooted. Note how *w*AnM and *w*AnD are present within a clade alongside *w*No and several assembled genomes of *Wolbachia* from *Drosophila mauritiana,* (green highlight). By contrast, previously sequenced *Wolbachia* of mosquitoes *w*Pip/*w*PipMol, and *w*AlbB, are present in separate clades.

***Figure 2*: Overview of identified orthogroups amongst *Wolbachia*. (A)** Graphical representation of set notation of 17 near-complete *Wolbachia* genomes from six of the main supergroups using UpsetR, and the protein orthologues that they encode. Each genome (one per row at the bottom half of the image) is treated as a 'set' containing a certain number of orthogroups (denoted by the bar graph on the bottom left of the image). The various permutations of intersections are denoted by the ball-and-stick diagram at the bottom of the image, and the size of these intersections denoted by the bar graph at the top of the image. *Wolbachia* genomes are colour-coded based on their supergroup organisation, with *w*AnM and *w*AnD sets highlighted by a red outline with no fill. Note how an intersect of all 17 *Wolbachia* genomes was identified as containing the vast majority of orthogroups- a 'core' proteome total of 523 orthogroups (first bar from left). All other subsequent permutations of intersects contain less than 53 orthogroups. There were no intersects that uniquely contained *w*AnM and *w*AnD, or uniquely contained only supergroup B *Wolbachia*. The inset stacked bar chart shows the distribution of singleton, i.e. genes that do not belong to an orthogroup, dark red bar segment, and strain-specific orthogroups, i.e. genes that belong to a orthogroup unique to that *Wolbachia* strain, light red segment. **(B)** Graphical representation of set notation of 27 supergroup B *Wolbachia* genomes, using the format as described for **(A)**. *Wolbachia* genomes includes eight existing published complete genomes, and 19

808 recently assembled genomes from Scholz et al., alongside the two recently assembled genomes *w*AnM
809 and *w*AnD (highlighted with a red box). Analysis was performed on local PGAP annotations of all 27
810 *Wolbachia* genomes. Note how the intersect of all 27 *Wolbachia* genomes shows a core proteome of
811 595 orthogroups, with the second largest intersect containing 221 orthogroups shared between the
812 Scholz et al. genome assembly for *Wolbachia* of *D. coccus* and an unidentified Insecta. There were no
813 intersects that uniquely contained *w*AnD and *w*AnM.

814 ***Figure 3:*** **Heatmap representation of presence-absence of various genes in metabolic and**
815 **secretion/transport system pathways amongst a selection of *Wolbachia* genomes.** The analysed
816 genomes are arrayed on the x-axis, with colours of the heatmap representing the various analysed
817 supergroups. The y-axis in turn represents different genes and metabolic pathways of interest to
818 Wolbachia studies. Greys in the heatmap represent an absence of a gene within the respective
819 genome. **(A)** Comparative illustration of 16 near-complete *Wolbachia* genomes. Column colours are
820 based on *Wolbachia* supergroup using a similar scheme to Figure 2, with columns representing the
821 genomes of *w*AnD and *w*AnM are highlighted with a more intense colour of the heatmap. These
822 genomes were observed to maintain all the genes and pathways common to supergroup B *Wolbachia*.
823 **(B)** Comparative illustration of 29 *Wolbachia* genomes of supergroup B. Columns are coloured based
824 on their origin, with blue columns being genomes from the study by Scholz *et al*. [44], and red being
825 genomes from existing *Wolbachia*, including *w*AnD and *w*AnM.

826 **Figure 4: BLAST Ring Image Generator (BRIG) visualisation of prophage regions in the genomes of**
827 ***w*No, *w*AnM and *w*AnD when compared to one another.** Each individual ring represents the BLAST
828 similarity score for a particular genome (represented by the different colours as defined by the key on
829 the right of panel A) against a template (represented by the innermost solid colour ring, and the name
830 at the centre of the circle). Differences in opacity of the rings represents the BLAST similarity score (as
831 represented by the key on the right of panel A), with solid colours representing 100% similarity, and
832 blank regions representing 0% similarity. The outer-most ring contains information on predicted

prophage and cif gene localisations **(A)** Comparison of *w*AnM and *w*AnD against a *w*No template genome. Note how the black bars representing predicted prophage regions by Ellegaard *et al*. [58] overlap areas with no similarity against the *w*AnM genome, whilst having some similarity to the *w*AnD genome. Also note how its single, intact *cif* gene pair is located separate from previously predicted prophage regions. **(B)** Comparison against a *w*AnM template genome. Note how this genome was noted to contain no prophage regions, and its single pseudogeised cif gene pair is located in an area with no similarity to both *w*No and *w*AnD. **(C)** Comparison against a *w*AnD template genome. Predicted prophage segments 1 and 2 were predicted by the PHASTER web server, with segment 3 predicted by Blastx searches against the prophage regions WOVitA1 and WOCauB1 through to B3, as identified by Bordentstein et al. [63]. Note how of the three predicted prophage regions, two showed similarity to the *w*No genome, and one showed no similarity to either genome. Also note how its two *cif* gene pairs are located separate from, but close to, predicted prophage segment 3. Also note how the intact *cif* gene pair appears within a region that shows weak to no similarity against both *w*AnM and *w*No.

Figure 5: **Maximum likelihood phylogenetic tree of concatenated *cif* gene nucleotide alignments, built following the methods of Martinez *et al*.** [14] **with 1,000 bootstrap replicates.** Only bootstrap values of over 80% are shown. The five types' of concatenated *cif* genes are highlighted with different colours, and their corresponding types annotated on them. Tree is midpoint-rooted. The two pairs of *cif* genes of wAnD were previously noted to be members of Type I and Type III, which is confirmed by this repeated analysis. The pair of *cif* genes in wAnM can be found in the well-supported Type II clade.

855 ***Figure 1***

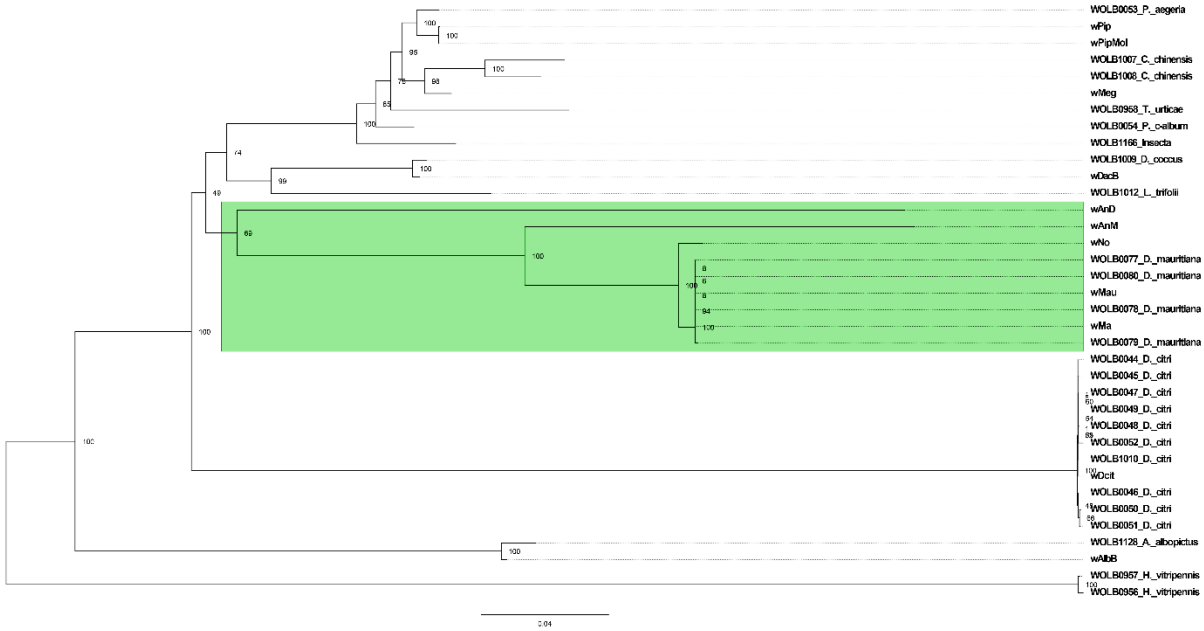

856

857

858 ***Figure 2***

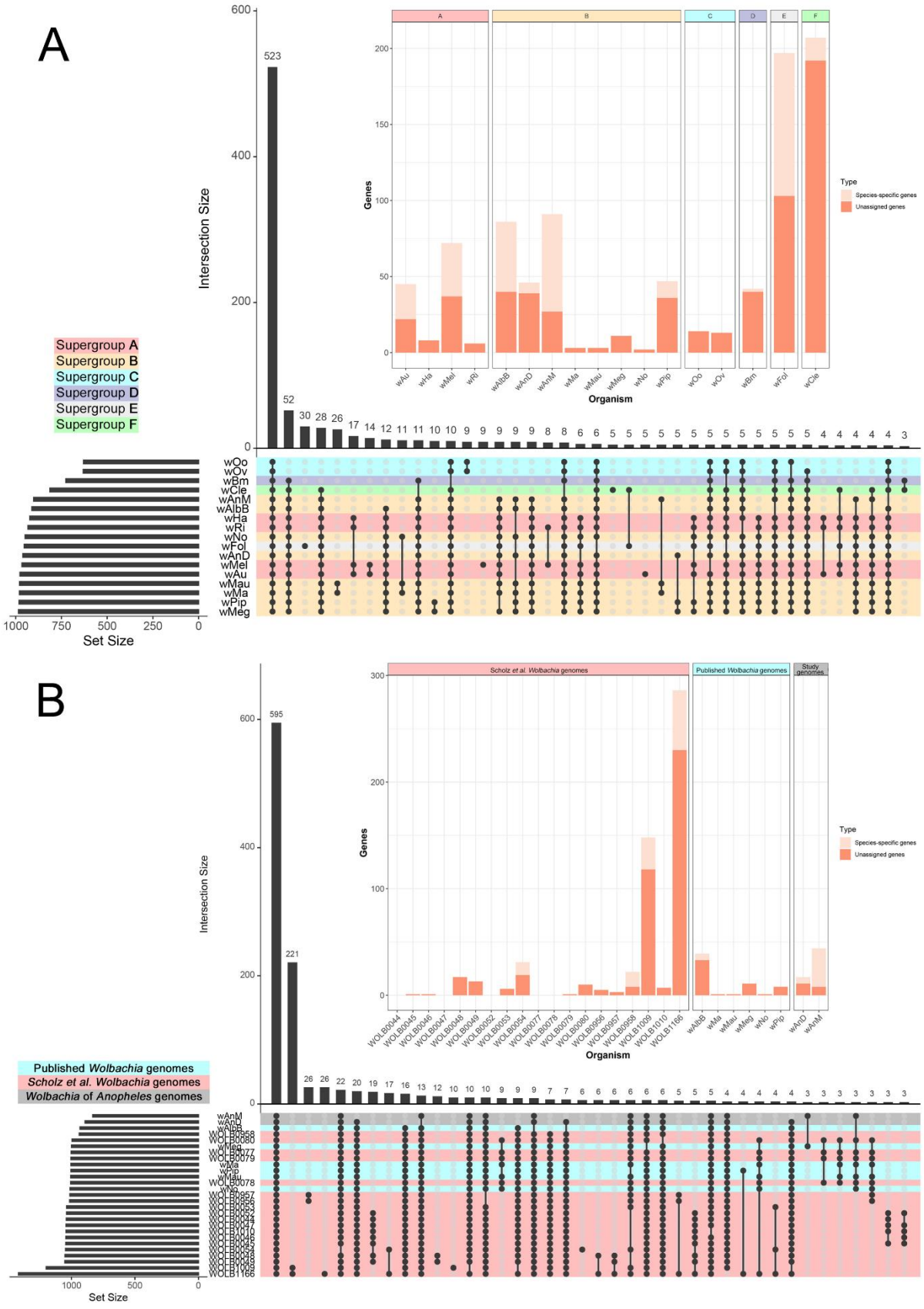

859

Figure 3

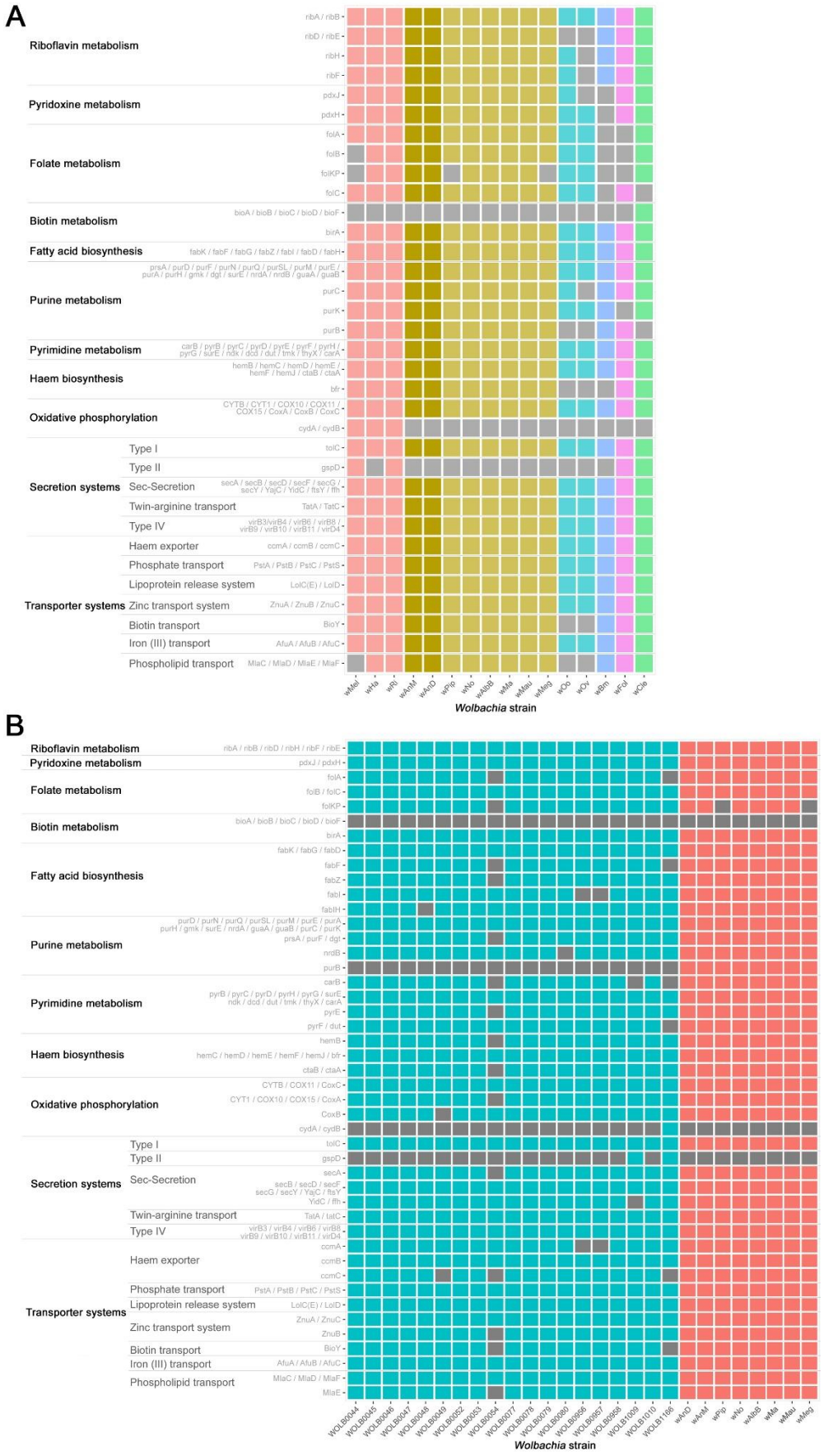

861

862 ***Figure 4***

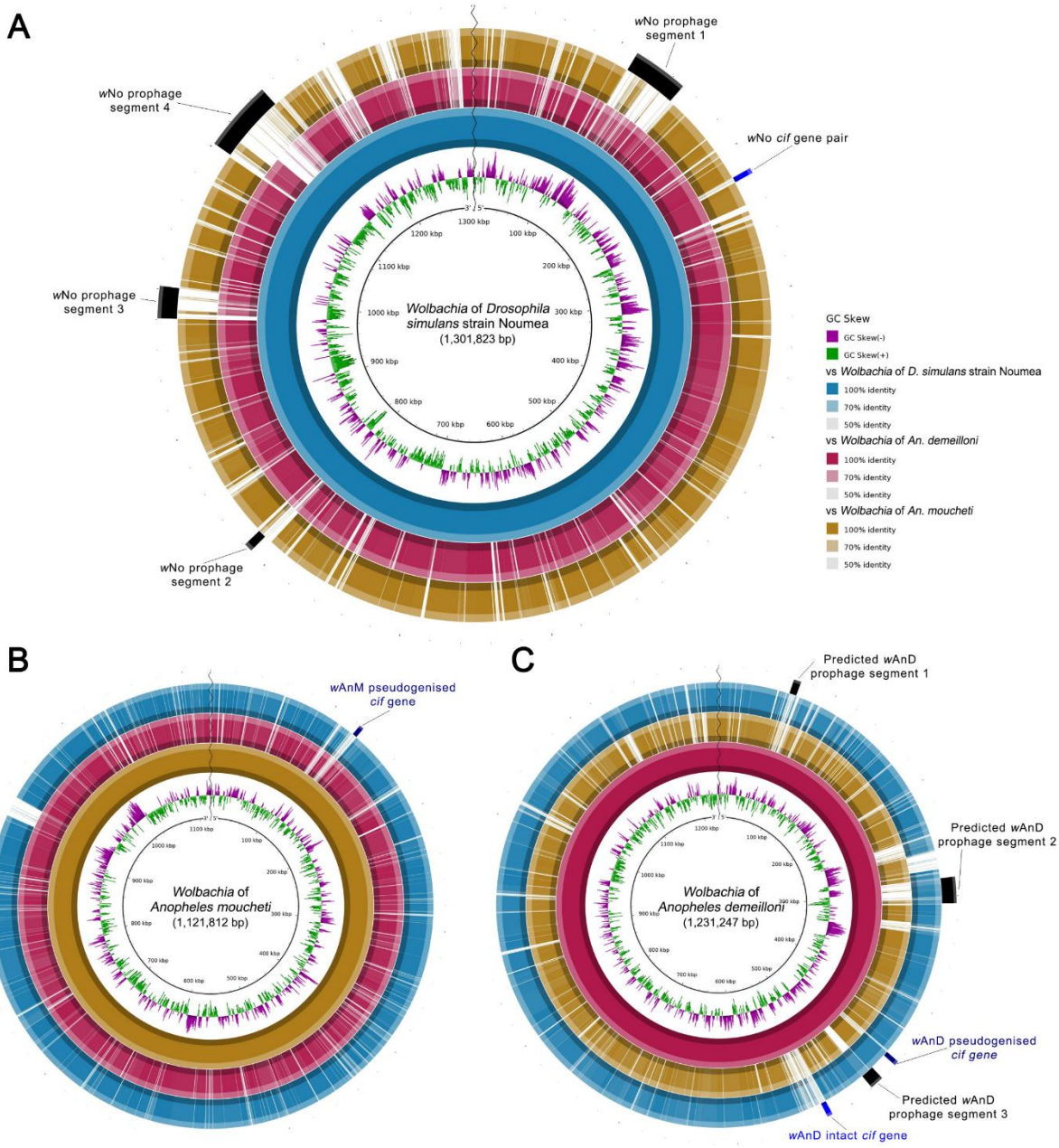

863

Figure 5

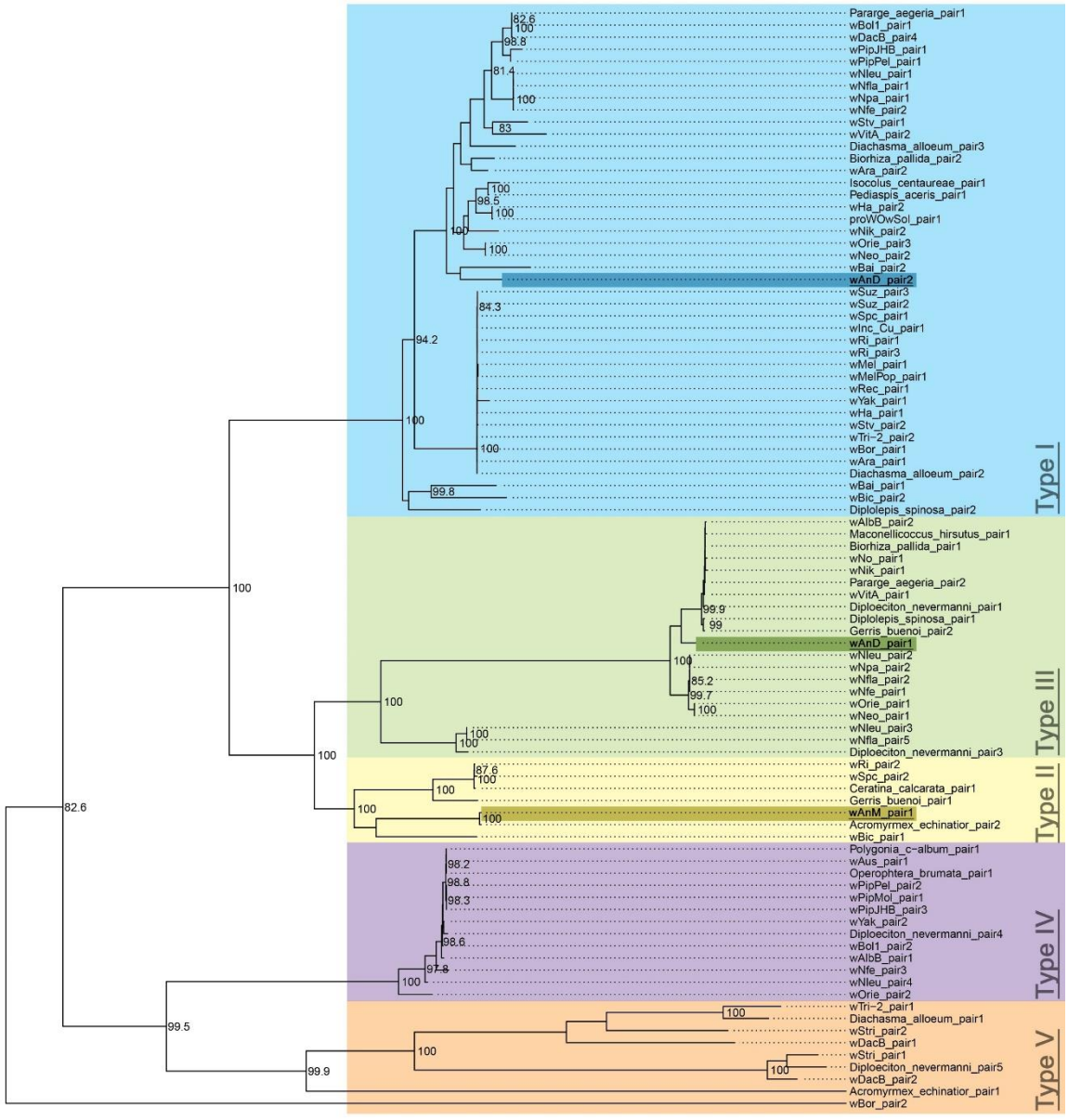

865

866 # Tables

Strain Name	Host organism	Supergroup	Size (Mb)	GC%	Total genes	Proteins	Pseudogenes	tRNA	rRNA	Other RNAs	Ankyrin proteins	BUSCO Score (out of 364)
***w*Au**	*Drosophila simulans*	A	1.27	35.22%	1,265	1,099	125	34	3	4	35	362 (99.5%)
***w*Ha**	*Drosophila simulans*	A	1.30	35.09%	1,242	1,110	91	34	3	4	36	362 (99.5%)
***w*Mel**	*Drosophila melanogaster*	A	1.27	35.23%	1,247	1,144	103	34	3	4	27	361 (99.2%)
***w*Ri**	*Drosophila simulans*	A	1.45	35.16%	1,340	1,245	95	35	3	4	33	360 (98.9%)
***w*AlbB**	*Aedes albopictus*	B	1.49	34.50%	1,442	1,180	221	34	3	4	38	355 (97.5%)
***w*AnD**	*Anopheles demeilloni*	B	1.23	33.58%	1,320	1,157	122	34	3	4	55	360 (98.9%)
***w*AnM**	*Anopheles moucheti*	B	1.12	33.59%	1,203	1,082	80	34	3	4	37	360 (98.9%)
***w*Ma**	*Drosophila mauritiana*	B	1.27	34.00%	1,196	1,055	100	34	3	4	49	360 (98.9%)
***w*Mau**	*Drosophila mauritiana*	B	1.27	34.00%	1,194	1,054	99	34	3	4	49	361 (99.2%)

wMeg	*Chrysomya megacephala*	B	1.38	33.95%	1,268	1,116	111	34	3	4	52	363 (99.7%)
wNo	*Drosophila simulans*	B	1.30	34.01%	1,208	1,062	105	34	3	4	53	363 (99.7%)
wPip	*Culex quinquefasciatus*	B	1.48	34.19%	1,385	1,241	103	34	3	4	63	362 (99.5%)
wOo	*Onochocerca ochengi*	C	0.96	32.07%	733	645	47	34	3	4	2	346 (95.1%)
wOv	*Onchocerca volvulus*	C	0.96	32.07%	734	648	45	34	3	4	3	345 (94.8%)
wBm	*Brugia malayi*	D	1.08	34.18%	1,029	845	143	34	3	4	18	357 (98.1%)
wFol	*Folsomia candida*	E	1.80	34.35%	1,662	1,541	79	35	3	4	94	362 (99.5%)
wCle	*Cimex lectularius*	F	1.25	36.25%	1,238	1,023	174	34	3	4	42	356 (97.8%)

Table 1: **Summary table of a selection of different near-complete *Wolbachia* genomes and their general genome properties.** Note the genomes of *w*AnD and *w*AnM (black box highlight), the similar genome properties compared to other *Wolbachia* genomes, but their relatively lower protein-coding gene number when compared against *Wolbachia* strains of supergroups A and B. BUSCO scores were calculated using the Rickettsiales_odb10 lineage, created on 2020-03-06 with a marker gene list total of 364.

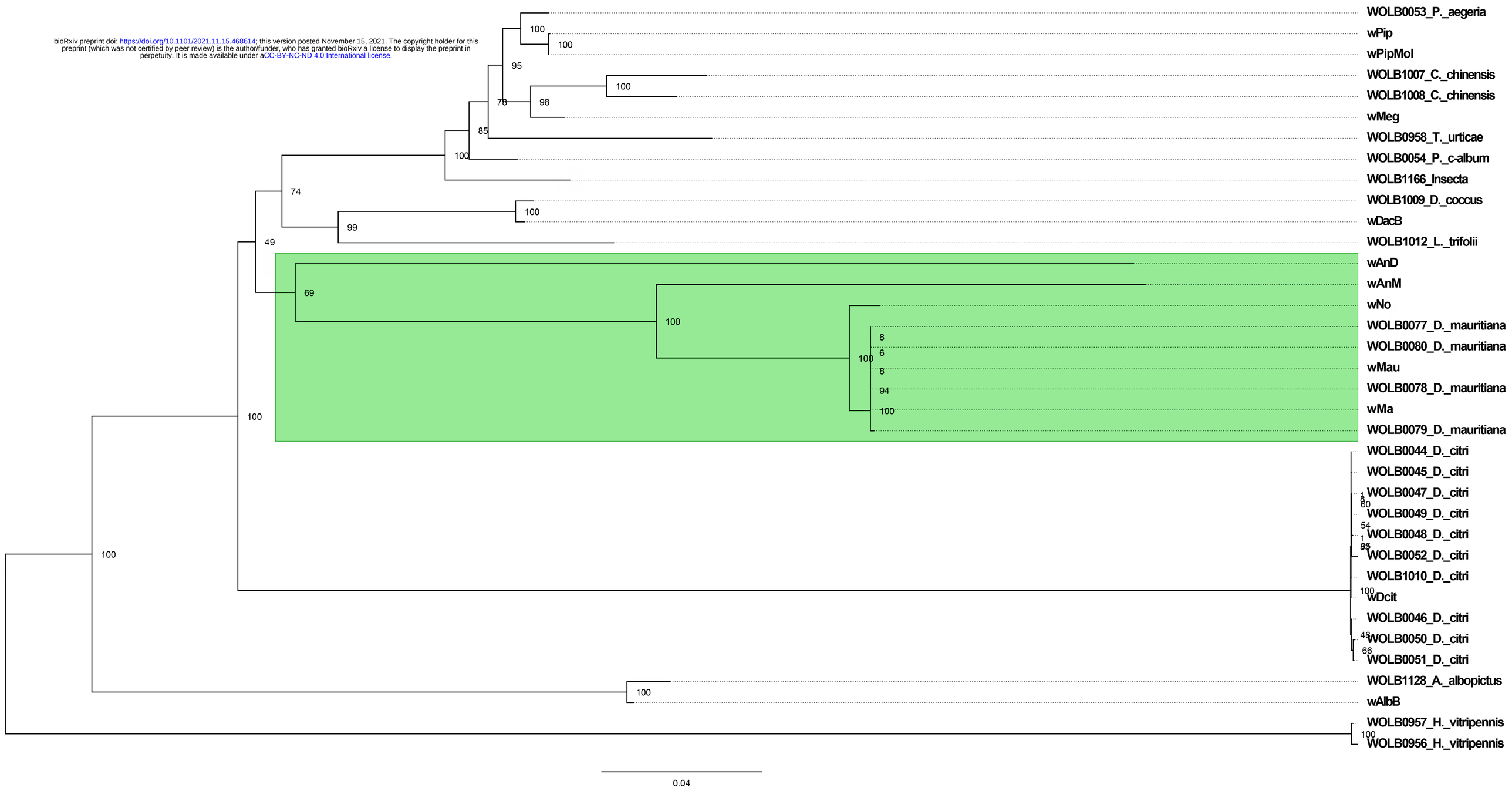

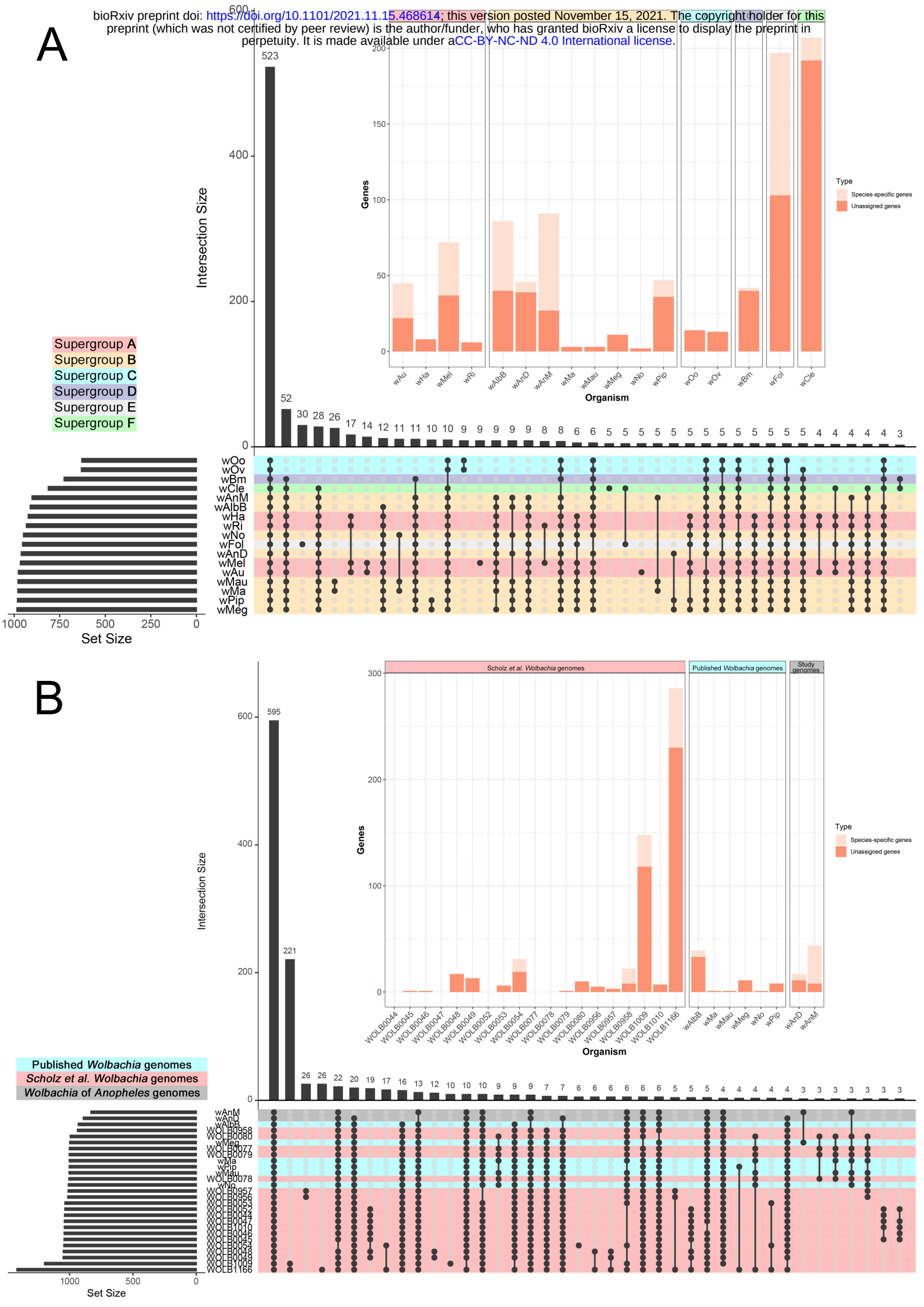

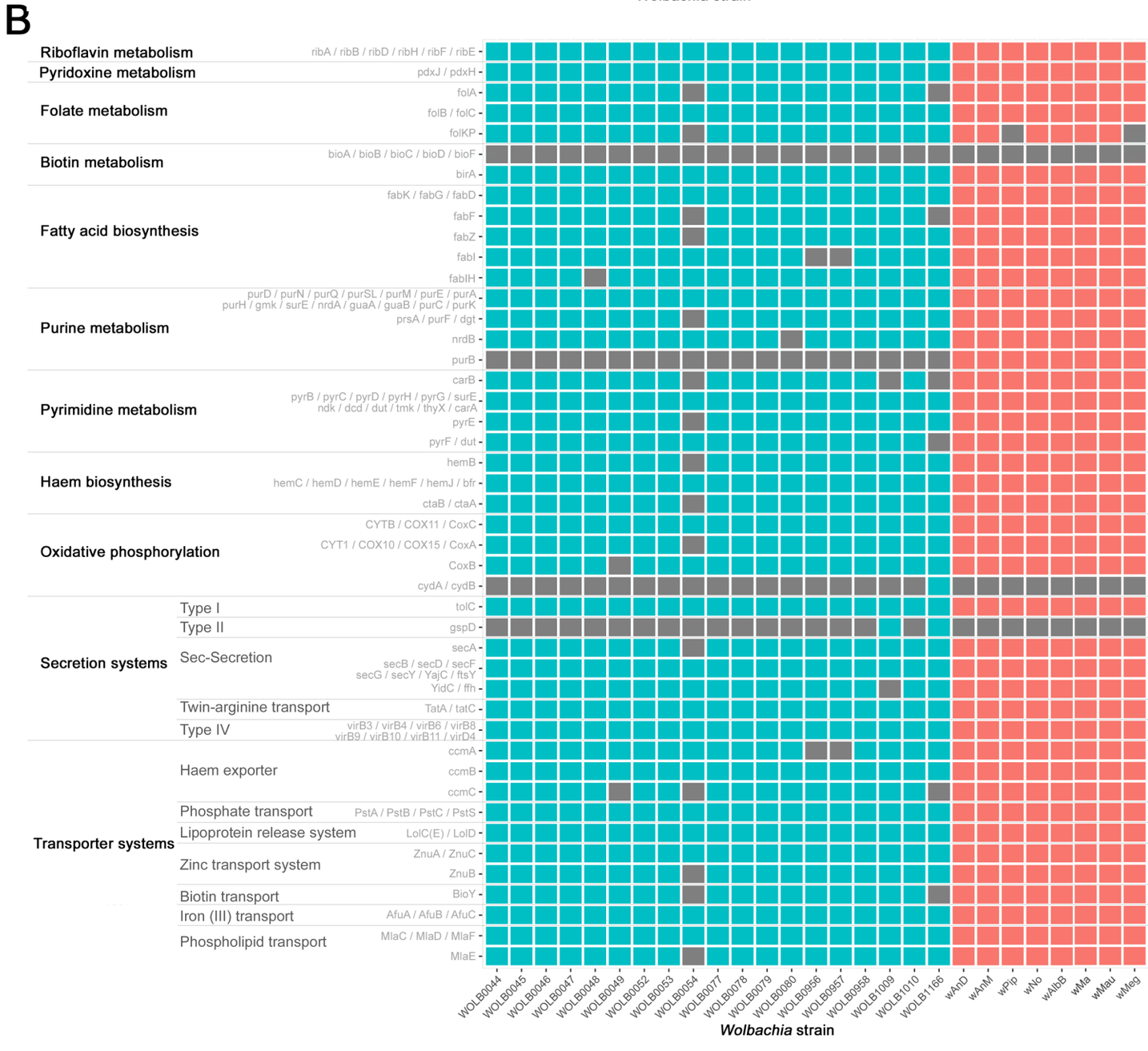

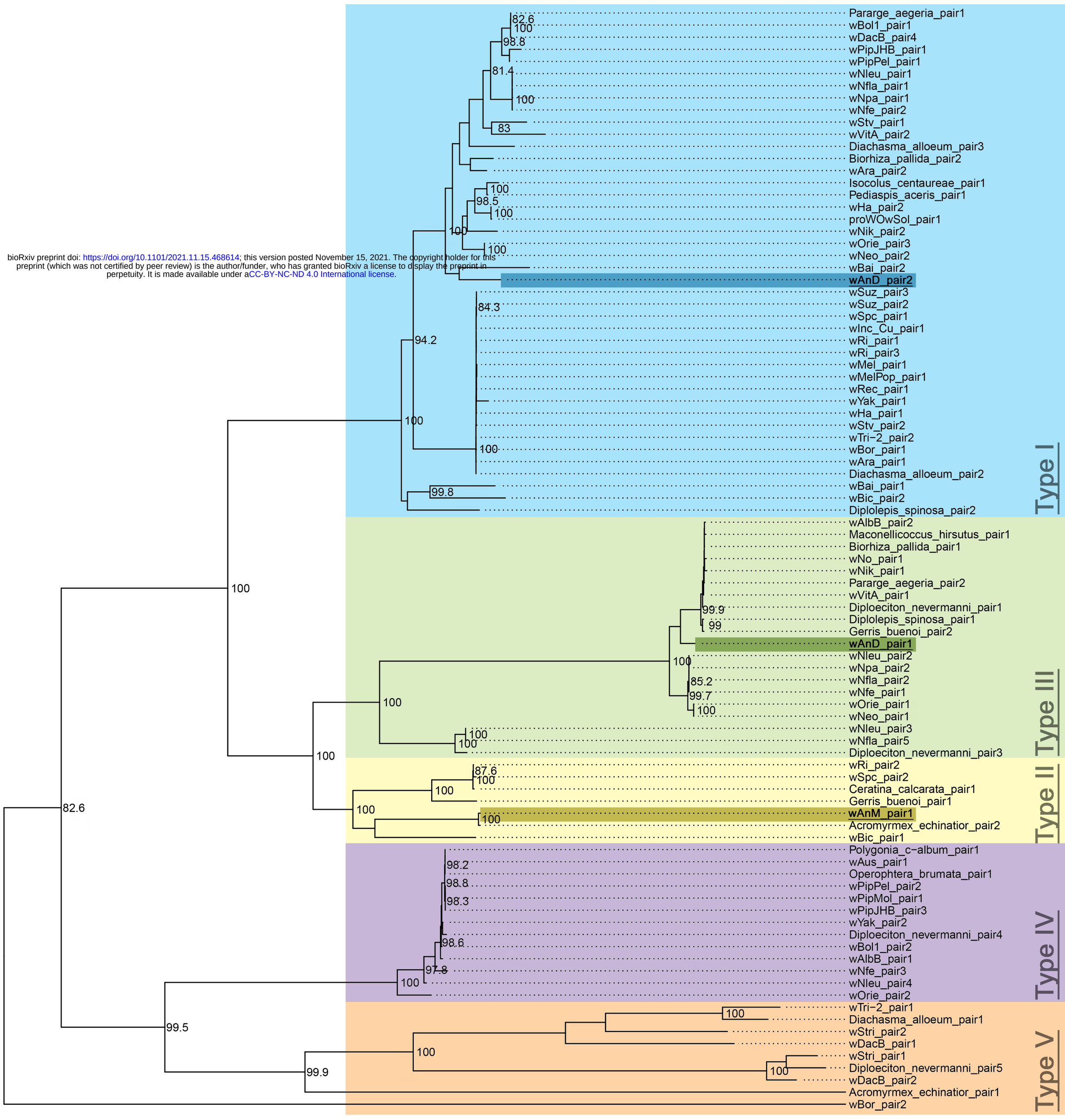

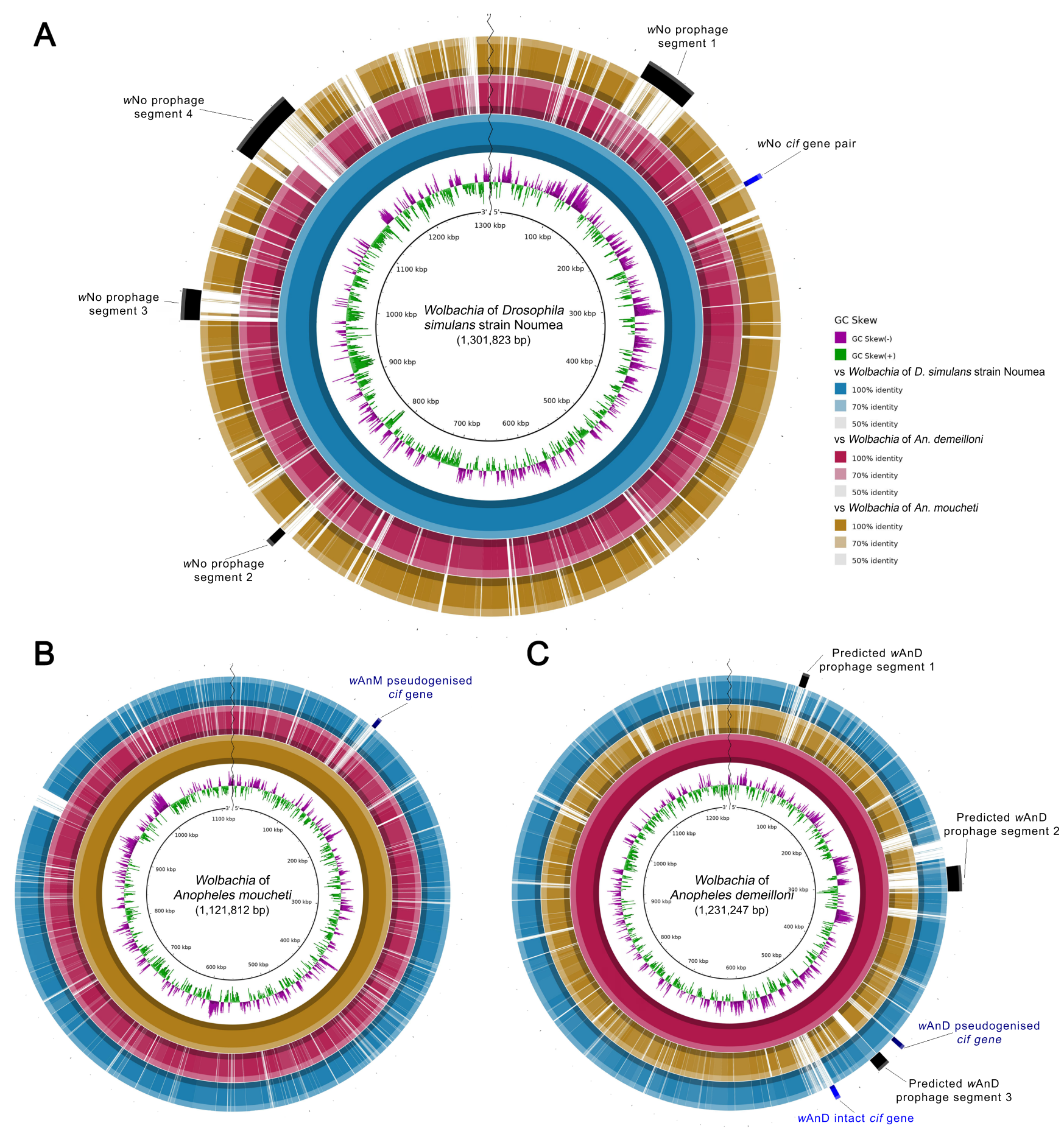
A
wNo prophage segment 1
wNo prophage segment 4
wNo cif gene pair
wNo prophage segment 3
wNo prophage segment 2
Wolbachia of Drosophila simulans strain Noumea (1,301,823 bp)
GC Skew
GC Skew(-)
GC Skew(+)
vs Wolbachia of D. simulans strain Noumea
100% identity
70% identity
50% identity
vs Wolbachia of An. demeilloni
100% identity
70% identity
50% identity
vs Wolbachia of An. moucheti
100% identity
70% identity
50% identity
B
wAnM pseudogenised cif gene
Wolbachia of Anopheles moucheti (1,121,812 bp)
C
Predicted wAnD prophage segment 1
Predicted wAnD prophage segment 2
Wolbachia of Anopheles demeilloni (1,231,247 bp)
wAnD pseudogenised cif gene
Predicted wAnD prophage segment 3
wAnD intact cif gene